The Thesis Committee for Yangyang Chen
Certifies that this is the approved version of the following thesis:

Hall Plot Analysis for Horizontal Well Injectivity

APPROVED BY
SUPERVISING COMMITTEE:

Supervisor: Kenneth Gray

Co-Supervisor: Hugh Daigle

Hall Plot Analysis for Horizontal Well Injectivity

by

Yangyang Chen, B.S.C.E

Thesis

Presented to the Faculty of the Graduate School of

The University of Texas at Austin

in Partial Fulfillment

of the Requirements

for the Degree of

Master of Science in Engineering

The University of Texas at Austin

May 2017

Dedication

To my beloved parents and grandmother.

Acknowledgements

First, I would like to express my deepest gratitude to my supervisor, Dr. Kenneth E Gray for offering me the opportunity to work with the Wider Windows Industrial Affiliate Program at The University of Texas at Austin. I truly appreciate his invaluable insights and consistent support throughout my study. I would also like to thank Dr. Hugh C. Daigle for being my co-advisor and giving me guidance and recommendations for this project.

I would like to thank all my colleagues and friends in our research group for all the insightful technical discussions.

I would like to thank Wider Windows sponsor companies for their financial support.

I would like to express my deepest gratitude to my mom, Lijuan Fan, and dad, Dong Chen, for always supporting and believing in me. They are the best parents and friends that I could ask for. I would also like to thank my grandma, Lipei Hu, for being my role model, encouraging me to learn, and sharing her wisdom with me.

I would like to thank my friends in Austin – Peidong Zhao, Pengpeng Qi, Bochao Zhao, Tianqi Deng, for being my company both in and outside of school. They have made my graduate school experience more memorable. I would also like to thank my friends back home in China for their moral support throughout these years.

Abstract

Hall Plot Analysis for Horizontal Well Injectivity

Yangyang Chen, M.S.E.

The University of Texas at Austin, 2017

Supervisor: Kenneth Gray

Co-Supervisor: Hugh Daigle

The Hall plot method, proposed by Howard Hall in the 1960s, is a widely-used tool for analyzing injectivity. Over the past decades, industry has been modifying the Hall plot method for applications in various scenarios such as formation damage and/or stimulation diagnosis, polymer injection, and gas injection. It has proved to be a simple, inexpensive, and effective way to diagnose changes in injectivity.

However, such applications are limited to vertical wells. This study proposes a new formulation of the Hall plot method for analyzing horizontal well injectivity. A numerical simulation model was built in CMG to verify the proposed method. The Hall plot method for horizontal well was then used to study various scenarios with different extents of formation damage, numbers of damaged skin zones, and reservoir anisotropy conditions. The works carried out in this study confirm the applicability of the Hall plot method on analyzing horizontal well injectivity.

Table of Contents

List of Tables

List of Figures

Chapter 1 Introduction

1.1 Objectives of This Research

The Hall plot method, proposed by Howard Hall in the 1960s (Hall, 1963), is a widely-used tool for analyzing injectivity. It is a plot of pressure integral versus cumulative injection volume. Ideally, by observing changes in the slope of a Hall plot, one can obtain information about changes in injection conditions. The Hall plot method has proved to be a simple, inexpensive, and effective way to analyze injectivity. Although there have been many applications and modifications based on the original Hall method, these previous studies are restricted to vertical wells. As horizontal drilling has become more advanced and widely-accepted over the past years, being able to analyze horizontal well injectivity is important for optimizing injection and production. Therefore, this research aims to modify the original Hall plot method, apply it to analyze horizontal well injectivity, and study the comparison between horizontal and vertical well injectivity under both isotropic and anisotropic conditions.

1.2 Brief Description of Chapters

In Chapter 2, the background and formulation of the Hall plot method is reviewed first, followed by a discussion of its advantages and disadvantages. Several applications and modifications of the conventional Hall plot, including diagnosing formation damage and/or fracture propagation, polymer injection, gas injection, and slope analysis method are revisited. Then, to formulate the Hall plot method for analyzing horizontal well water injectivity, basic horizontal well theories are discussed.

In Chapter 3, based on the theories reviewed in Chapter 2, the study derives a Hall plot method for horizontal wells. Simulation models that are used to verify the applicability of the method are delineated.

In Chapter 4, details on analyzing the simulation results using the Hall plot method are discussed. In addition, horizontal versus vertical well injectivity is compared using Hall plots, for both isotropic and anisotropic reservoirs. In Chapter 5, results, conclusions, and recommendations are briefly summarized.

Chapter 2: Literature Review

2.1 Conventional Hall Plot Method

Hall plot, proposed by Howard Hall in the 1960s, has been a simple and useful tool for monitoring the performance of an injection well. The main purpose of Hall's work is to eliminate complications caused by varying pressure and injection rate. On the conventional Hall plot, the integral of surface injection pressure with respect to time is plotted against the cumulative water injection volume to monitor changes in injection conditions. The original Hall's method was developed for steady-state, single phase, radial flow of a Newtonian fluid to a vertical wellbore.

Hall started with using Darcy's equation for single phase, steady-state, Newtonian flow of a well centered in a circular reservoir:

$$q = \frac{k_{rw} kh(P_{wf} - P_e)}{141.2 B_w \mu_w [\ln\left(\frac{r_e}{r_w}\right) + s]}, \qquad (2.1)$$

where q is the water rate in STB/day, k_{rw} is the water relative permeability, k is the absolute permeability in mD, h is the reservoir thickness in ft, P_{wf} is the wellbore pressure in psi, P_e is the reservoir pressure in psi, B_w is the dimensionless formation volume factor, r_w is the wellbore radius in ft, and r_e the radius at water-oil front in ft, s is the skin factor (Hall, 1963).

Hall assumed that P_e is constant over short periods and that $\ln(r_e/r_w)$ can also be treated as a constant. Hall integrated both sides with respect to time to get

$$W_i = \frac{k_{rw} kh \int (P_{wf} - P_e) dt}{141.2\ B_w \mu_w [\ln\left(\frac{r_e}{r_w}\right) + S]}, \qquad (2.2)$$

where W_i represents the cumulative water injected in barrel. He then used the relationship between wellhead pressure, hydrostatic pressure, and pressure drop in tubing:

$$P_{wf} = P_{tf} + H\rho_w - \Delta P_t. \qquad (2.3)$$

$(H\rho_w - \Delta P_t)$ is considered constant so that only P_{tf} varies with time. Equation 2.2 can then be written as

$$\int P_{tf}dt = \frac{141.2\ B_w\mu_w[\ln\left(\frac{r_e}{r_w}\right)+S]}{k_{rw}kh} W_i + \int (P_e + \Delta P_t - H\rho_w)dt. \qquad (2.4)$$

For simplicity, Hall dropped the second term on the right-hand side of Equation 2.4 and plotted the left-hand side, the integral of wellhead pressure with respect to time, versus cumulative injection. The plot came to known as the Hall plot, which is shown in Figure 2.1. By plotting in this format, it can be observed that the plot is a straight line with slope

$$m_H = \frac{141.2\ B_w\mu_w[\ln\left(\frac{r_e}{r_w}\right)+S]}{k_{rw}kh}. \qquad (2.5)$$

As shown in Figure 2.1, the straight line represents the injectivity of an undamaged situation, where the skin factor S equals to zero in the expression of the slope m. If an injection well is stimulated, the slope decreases, and if a well is damaged, the slope increases.

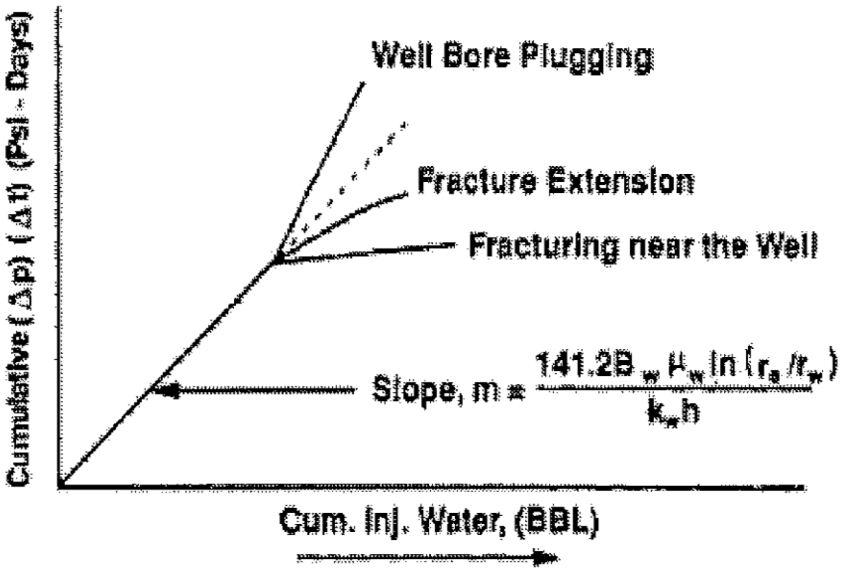

Figure 2.1: Hall Plot. (Buell et al. 1990)

2.2 THE ADVANTAGES AND DISADVANTAGES OF THE HALL PLOT

Hall's method has several advantages. First of all, since the Hall plot is a steady-state analysis method and a continuous monitoring technique, it is capable of identifying changes in injection characteristics that occur over an extended period of time (Buell, 1990). This characteristic separates Hall's method from other transient methods such as falloff tests, injection tests, and type-curve analysis, all in which the reservoir properties are determined at one point in time. Secondly, integrating the pressure data ($\int(P_{wf} - P_e)dt$) has a smoothing effect, which filters out short-term fluctuations of pressure and rate. Thirdly, data acquisition for generating a Hall plot is inexpensive, as only the recording of surface pressure and cumulative injection are required. Accounting for hydrostatic head and friction loss, surface pressure can then be converted to bottom hole pressure. On the other hand, transient methods, such as injection and falloff tests, normally require running gauges on wireline to depth, which could be much more expensive.

However, in the conventional Hall's method, the skin factor and transmissibility terms are combined in the slope. As a result, it is impossible to determine both parameters using a Hall plot if neither of them is known. Often, to use a Hall plot effectively, running falloff or injection tests periodically is still required in order to determine individual values of transmissibility and skin (Buell, 1990).

2.4 APPLICATIONS AND MODIFICATIONS OF CONVENTIONAL HALL PLOT METHOD

Since Hall proposed the original Hall's method, industry has been applying and modifying the technique to monitor injectivity in various conditions. Several important extensions of the original Hall's method are reviewed in this section.

2.4.1 Polymer Injection

With the advance in enhanced oil recovery using polymer and micellar solutions, the injectivity of such solutions has become of interest to the industry. The interpretation of injection pressures and rates associated with polymer and/or micellar solution injection is important to the efficient application of the solutions (Buell et al. 1990). In 1990, Buell et al. demonstrated that the Hall plot can also be applied to analyze injectivity of polymer solutions and that in-situ and residual resistance factors of a polymer solution can be determined using this modified Hall method.

As a waterflood begins, two-phase flow exists in the near-wellbore region, where water and oil banks form. Applying Darcy's law in a series manner, the slope of the Hall plot for a water and oil bank can be expressed as

$$m_H = \left(\frac{141.2}{kh}\right)\left\{\frac{\mu_w B_w\left[\ln\left(\frac{r_{b1}}{r_w}\right)+s\right]}{k_{rw}} + \frac{\mu_o B_o\left[\ln\left(\frac{r_e}{r_{b1}}\right)+s\right]}{k_{ro}}\right\}, \tag{2.6}$$

where r_{b1} is the interface between the oil and water banks and can be estimated from the Buckly-Leverett equation in radial coordinates:

$$r_{b1}^2 = \frac{5.615 W_i}{\emptyset \pi h}\left(\frac{\partial f_w}{\partial S_w}\right)_F + r_w^2. \tag{2.7}$$

Due to the logarithmic nature of Equation 2.6, the water bank term will dominate when the oil bank is pushed away from the wellbore. Using a similar method, Buell et al. (1990) developed an equation for when the injected fluid is a non-Newtonian fluid, such as a polymer solution:

$$m_H = 141.2\left\{\frac{\mu_w B_w\left[\ln\left(\frac{r_{b2}}{r_w}\right)+s\right]}{hk_a k_{rw}} + \frac{\mu_p B_w\left[\ln\left(\frac{r_{b1}}{r_{b2}}\right)+s\right]}{hk_a k_{rp}} + \frac{\mu_o B_o\left[\ln\left(\frac{r_e}{r_{b1}}\right)+s\right]}{hkk_{ro}}\right\}. \tag{2.8}$$

Three fluid banks – water, polymer, and oil – are assumed to be present in the near-wellbore region. Subsequently, by introducing the resistance factor, R_f, and residual resistance

factor, R_{rf}, Equation 2.8 can be expressed with one absolute permeability and aqueous-phase viscosity. R_f and R_{rf} are defined as

$$R_f = \frac{water\ mobility}{polymer\ mobility} = \frac{(kk_{rw})/\mu_w}{(k_a k_{rp})/\mu_p}, \qquad (2.9)$$

$$R_{rf} = \frac{absolute\ permeability\ before\ polymer}{absolute\ permeability\ after\ polymer} = \frac{k}{k_a}. \qquad (2.10)$$

Substituting Equation 2.9 and Equation 2.10 into Equation 2.8, Buell et al. (1990) obtained the following expression:

$$m_H = 141.2\left\{\frac{R_{rf}\mu_w\left[\ln\left(\frac{r_{b2}}{r_w}\right)+s\right]}{hkk_{rw}} + \frac{R_f\mu_w B_w \ln\left(\frac{r_{b1}}{r_{b2}}\right)}{hkk_{rw}} + \frac{\mu_o B_o \ln\left(\frac{r_e}{r_{b1}}\right)}{hkk_{ro}}\right\}. \qquad (2.11)$$

In Equations 2.8 and 2.11, the non-Newtonian rheology is ignored so that apparent viscosity can be assumed to be constant through space. By demonstrating the method with field data, it was shown that the actual change in apparent viscosity through space is relatively small and can be approximated by a constant. Buell et al. (1990) also pointed out that when the bank in contact with the wellbore has moved out a substantial distance, the other terms can be dropped without significant error, and that the bank in contact with the wellbore can be assumed to extend to the drainage radius. As a result, in Equation 2.11, the three terms can be evaluated individually to determine whether the bank in contact with the wellbore will dominate and rearranged to account for any injection sequence (Buell et al., 1990).

2.4.2 Gas Injection

The process of gas flow through porous media is complicated due to the complexity of gas compressibility, pressure dependence of properties, and relative permeability variations during injection (Talabi, 2016). Talabi (2016) investigated the applicability and modifications of the Hall plot method for gas injection, particularly for the "single-phase

gas injection into a gas phase" case. More specifically, two formulations – one high-pressure and one low-pressure – were derived and verified using a numerical model.

For the low-pressure gas injection case, Talabi arrived at a modified Hall plot expressed as

$$\sum\left[\frac{(P_{wi}^2-P_R^2}{\bar{\mu}\bar{z}}\Delta t\right]=\frac{Q_g}{C_1}, \qquad (2.12)$$

where P_{wi} is the injection well bottom hole pressure, P_R is the average reservoir pressure, $\bar{\mu}$ is the viscosity evaluated at $\bar{P}$, $\bar{z}$ is the gas compressibility factor evaluated at $\bar{P}$, $\bar{P}$ is the average of reservoir and bottom hole pressures, Q_g is the cumulative gas injection volume, and C_1 is a constant equal to 0.000707kh/T. Equation 2.12 can then be plotted as a straight line with slope $1/C_1$ (Talabi, 2016). For the high-pressure gas injection case in which the pressures are typically above 4,000 psia, Talabi (2016) derived the modified Hall plot expression as

$$\sum(P_{wi}-P_R)\Delta t=\frac{Q_g}{2C_2} \qquad (2.13)$$

where C_2 is a constant equal to $\frac{\bar{P}}{\bar{\mu}\bar{z}}$. Equation 2.13 can then be plotted as a straight line with slope $1/2C_2$ (Talabi, 2016). The modified Hall method for low- and high-pressure gas injection scenarios were verified using reservoir simulation. Figure 2.2 and 2.3 show the modified Hall plots for low- and high-pressure approximations. In both cases, the modified Hall plots remove the nonlinearity in compressibility and viscosity associated with gas flow; and only true change in skin is indicated by a change in slope (Talabi, 2016).

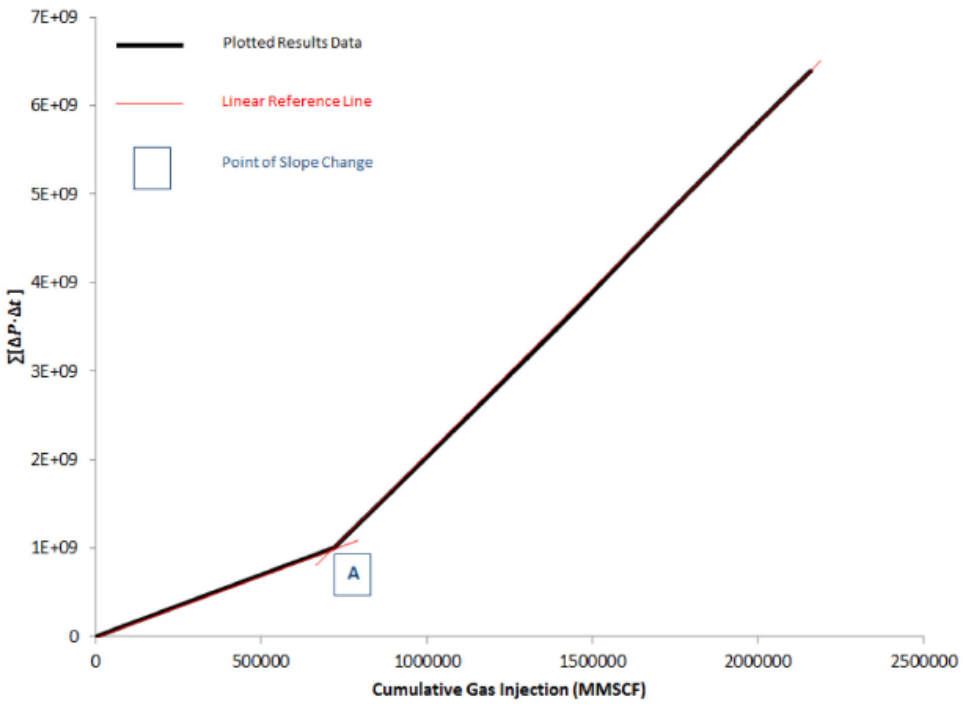

Figure 2.2: Modified Hall plot for low-pressure gas injection (Talabi, 2016).

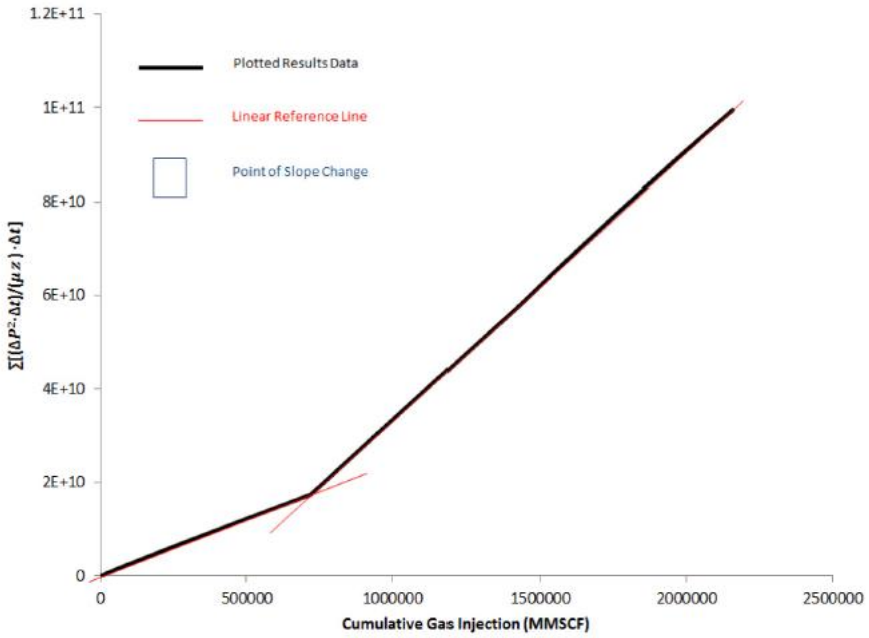

Figure 2.3: Modified Hall plot for high-pressure gas injection (Talabi, 2016).

2.4.2 Modified-Hall Plot Methods

Based on the conventional Hall's method, Silin et al. (2005) proposed a new method called slope analysis. This method analyzes the variation of the slope of the plot of the time integral of pressure versus cumulative injection volume. More specifically, the slope analysis gives an estimate of an apparent reservoir pressure, which is subsequently used to correct the Hall plot analysis or to map the average reservoir pressure over several patterns or an entire waterflood project (Silin et al., 2005).

Silin et al. (2005) pointed out that, the simplicity of Hall's method can be deceiving. In fact, an accurate Hall plot interpretation requires knowledge about the reservoir pressure at the distance equal to the mean influence radius of the well (Silin et al., 2005). Therefore, if Hall's method is applied without knowing the effective ambient reservoir pressure, the interpretation of changes in Hall slope may be incorrect. To address this issue, Silin et al. (1990) started by analyzing the Hall plot to extract information on the effective reservoir pressure, P_e, and well injectivity. They first denoted the Hall integral and cumulative water injection as

$$\Pi(t) = \int_{t_0}^{t} P_w(\tau)d\tau \text{ and } V(t) = \int_{t_0}^{t} Q(\tau)d\tau. \qquad (2.14)$$

To calculate the slope of the Hall plot, one needs to evaluate the derivative

$$S = \frac{d\Pi}{dV}. \qquad (2.15)$$

From Equation 2.12, S can be expressed as

$$S = \frac{P_w}{Q}. \qquad (2.16)$$

Under steady-state radial flow, downhole wellbore pressure P_w can be expressed as

$$P_w = P_e + bQ, \qquad (2.17)$$

where $b = \frac{\mu}{2\pi kH} ln \frac{r_e}{r_w}$. Then, from Equation 2.14 and 2.15, at quasi steady-state conditions,

$$S = \frac{P_e}{Q} + b. \qquad (2.18)$$

Equation 2.16 implies that the slope of S is a linear function of 1/Q. Since injection rate Q and slope S can be directly obtained from measurement, both the ambient reservoir pressure, P_e and the well injectivity parameter, b, can be obtained from Equation 2.16 by linearly fitting the plot of S versus 1/Q. Silin et al. (2005) named this method *slope analysis*. Figure 2.2 and 2.3 show a set of simulated injection rate and pressure data that can be analyzed using the slope analysis method. As shown in Figure 2.4, the vertical jumps in the slope plot indicate step increase of injection rate. Since the displacements are parallel, they express changes in the injectivity parameter b. Silin et al. (2005) pointed out that, given that the formation properties did not change in these simulated data, the changes in b were entirely due to the expansions of the influence zone radius caused by the increasing injection rate and pressure. Furthermore, the ambient reservoir pressure, P_e, estimated from the slope plot is less than 1% different from the exact ambient pressure used in these simulations, proving the applicability of slope analysis method (Silin et al., 2005).

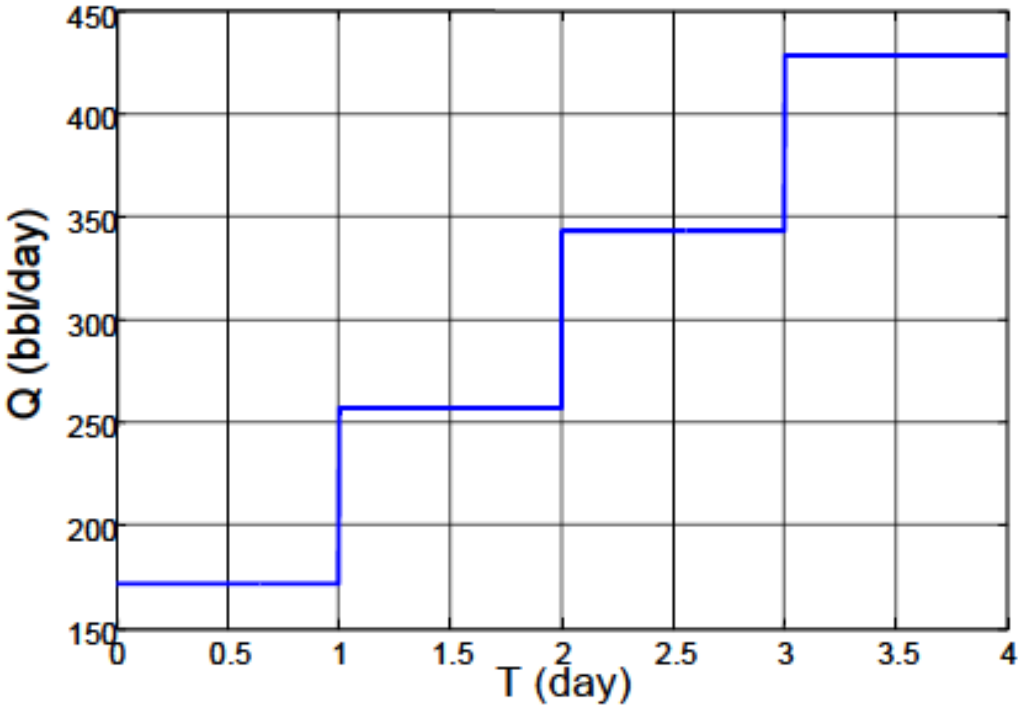

Figure 2.4: Injection rate with step increase. (Silin et al., 2005)

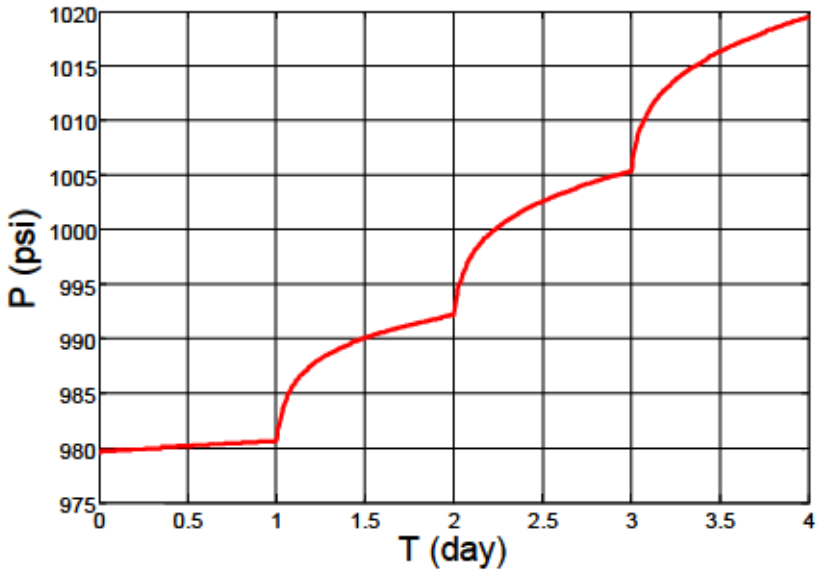

Figure 2.5: Computed pressure profile corresponding to injection rate. (Silin et al., 2005)

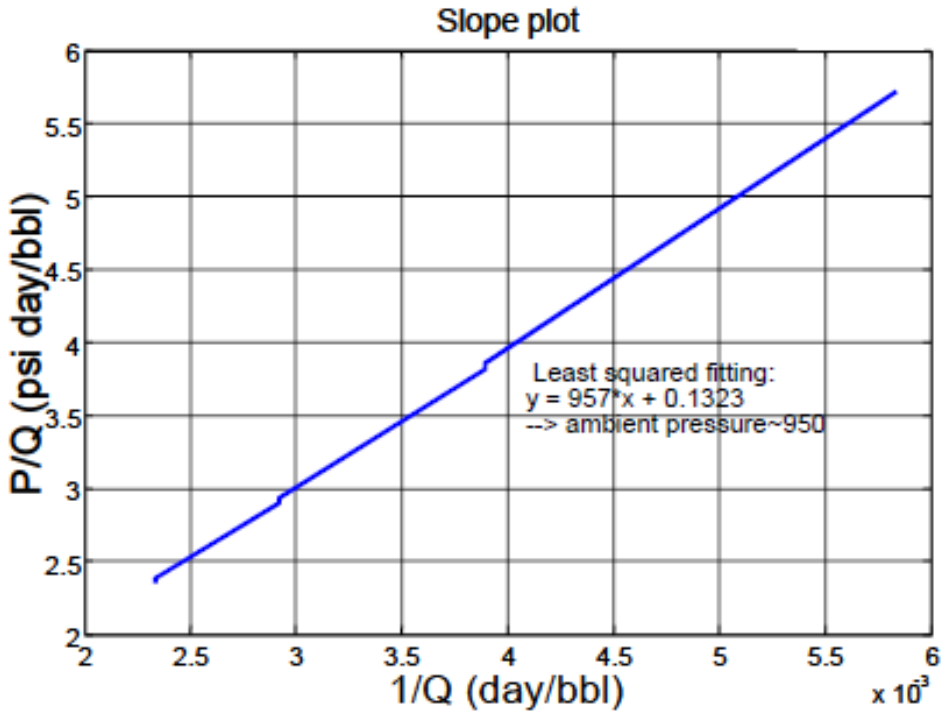

Figure 2.6: Slope plot analysis. (Silin et al., 2005)

Izgec and Kabir (2009) presented a reformulation of the Hall method involving updating the outer-bank pressure, or P_e, at every time step using transient and pseudosteady-state approaches. Additionally, they demonstrated that comparing and contrasting the derivative curve with the Hall integral could provide definitive clues on fracturing, nonfracturing, and plugging of the formation. More specifically, two curves trace the same path in matrix-dominated flow without fracturing or formation plugging. The derivative curve separates downward from the Hall curve in a fracturing condition and upward in a formation plugging condition. Figure 2.7 demonstrates the application of the Hall plot and its derivative plot on identifying change in injection conditions. In this case, Phase I represents early-time matrix injection, followed by formation plugging in Phase II;

finally, in Phase III, the formation is fractured as seen from the downward separation of the derivative curve from the Hall plot (Izgec and Kabir, 2009).

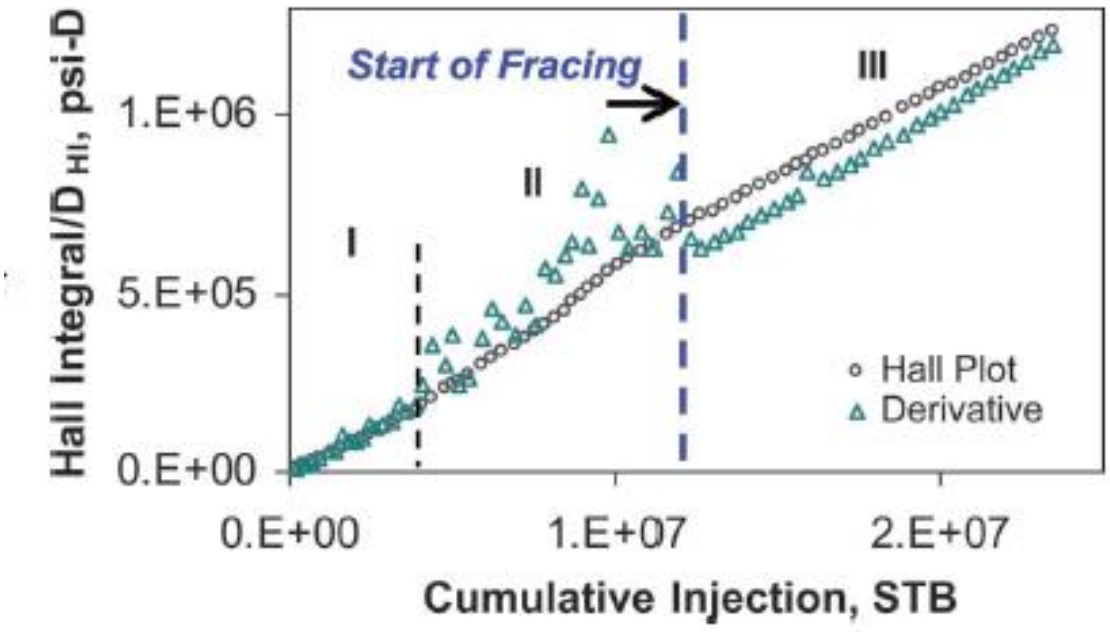

Figure 2.7: Normal injection, plugging, and fracturing identified. (Izgec and Kabir, 2009)

Izgec and Kabir (2009) first used the pseudosteady-state approximation to calculate pressure inside the waterbank, which is expressed as

$$P_e = P_{wf} - \frac{i_w B\mu}{2\pi kh}\left[\frac{r_o^2}{(r_o^2 - r_w^2)}\ln\left(\frac{r_e}{r_w}\right) - \frac{1}{2}\frac{(r_e^2 - r_w^2}{(r_o^2 - r_w^2)} + s^*\right], \qquad (2.19)$$

where i_w is the water-injection rate in STB/D,r_o is the outer reservoir radius in ft, s^* is the dimensionless pseudoskin. r_e, the water-bank radius in ft, can be calculated using

$$r_e = \left(\frac{5.615 W_i B}{\pi h \emptyset (1 - S_{or})}\right)^{1/2}, \qquad (2.20)$$

where S_{or} is the residual oil saturation, W_i is the cumulative water injection in STB, and $\emptyset$ is the porosity of the reservoir. Using the line-source solution for transient flow during

injection, it was shown that pseudoskin can be updated continuously with the following equation

$$s^* = \frac{1}{0.868}\left[\frac{b}{m} - \log\left(\frac{k}{\emptyset\mu c_t r_w^2}\right) + 3.23\right], \qquad (2.21)$$

where m is the semilog slope in psi/log-cycle and equals to $162.6B\mu/kh$.

A series of steps were proposed for generating the diagnostic graphs for Hall integral and its derivative. Izgec and Kabir (2009) summarized the methodology as the following:

1. Calculate s^* with Equation 2.21.
2. Calculate cumulative injection.
3. Calculate water-bank radius r_e with Equation 2.20.
4. Calculate water-bank pressure P_e with Equation 2.19.
5. Calculate numeric derivative of the Hall integral using

$$D_{HIn} = \frac{d\int(p_{wf}-p_e)dt}{dln(W_i)} \cong \frac{I_H^{n+1}-I_H^n}{\ln(W_i)^{n+1}-\ln(W_i)^n}, \qquad (2.22)$$

where $I_H = \int(p_{wf} - p_e)dt$.

This modification of the Hall's method was proven to be much more discriminating for yielding the desired diagnostic clues when applying to field examples. The reformulation of the injection bank and pressure at the water/oil interface makes the diagnostic plots more robust and appropriate for pre- and post-breakthrough situations. Also, when using the Hall integral and its derivative curve together, unambiguous diagnosis of a well's performance status can be obtained (Izgec and Kabir, 2009).

2.5 HORIZONTAL WELL THEORIES

2.5.1 Introduction

As stated, the conventional Hall's method was developed based on a vertical wellbore. In this research, in order apply Hall's method on horizontal wells, it is important to first review theories of horizontal wells. As shown in Figures 2.8 and 2.9, a vertical well drains a cylindrical volume, whereas a horizontal well drains a three-dimensional ellipse, which is expected to have a larger volume than a vertical well. Figure 2.10 shows a vertical well with a fully penetrating and infinite conductivity fracture that covers the entire reservoir height, h. A horizontal well, shown in Figure 2.11, then can be considered as a special case of the fractured vertical well if the height of the fracture is reduced to the horizontal wellbore diameter (Joshi, 1991).

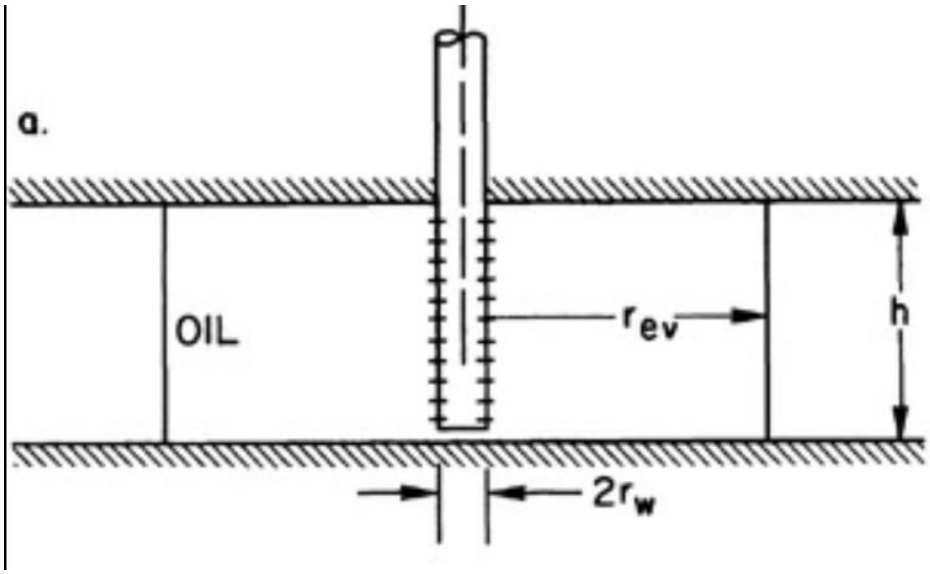

Figure 2.8: A schematic of vertical well drainage area. (Joshi, 1991)

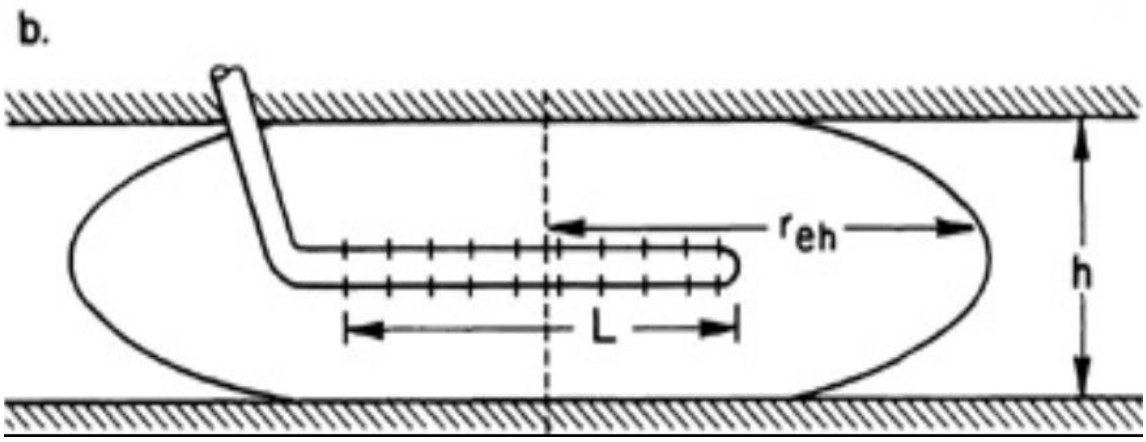

Figure 2.9: A schematic of horizontal well drainage area. (Joshi, 1991)

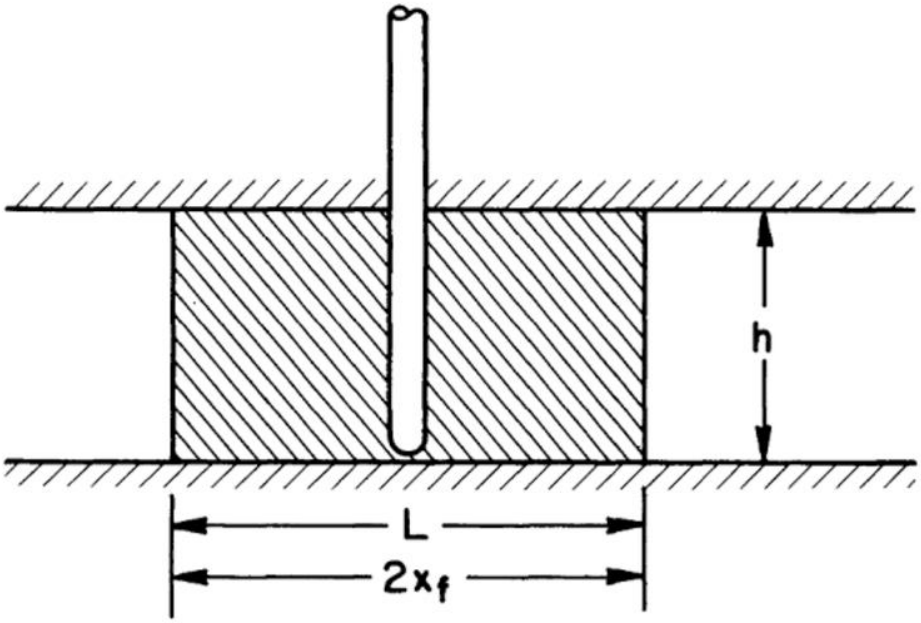

Figure 2.10: A schematic of a fractured vertical well. (Joshi, 1991)

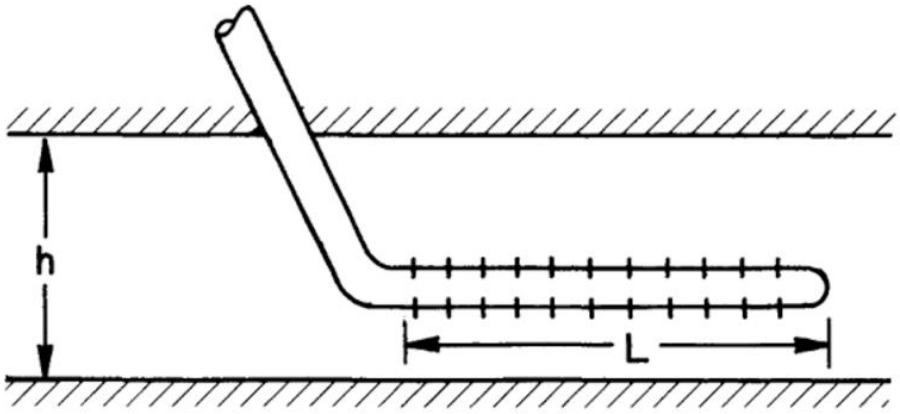

Figure 2.11: A schematic of a horizontal well. (Joshi, 1991)

2.5.2 Skin Factor

The concept of skin factor was first introduced to the petroleum industry by Van Everdingen and Hurst (1949) when they noticed that the measured bottom-hole flowing pressure was less than the calculated theoretical value for a given flow rate (Joshi, 1991). This pressure drop was found to be associated with a small zone of changed permeability around the wellbore caused by formation damage. Van Everdingen and Hurst associated pressure drop as a skin factor effect and defined the skin pressure drop in damaged wells as

$$s = \frac{kh(\Delta p)_{skin}}{141.2q\mu_o B_o}. \qquad (2.23)$$

This definition, however, only works well in damaged wells. When the skin factor is negative, fluid flows from the wellbore into the formation and incurs mathematical and physical difficulties in interpreting Equation 2.23. To overcome this problem, Hawkins introduced another expression of the skin factor in terms of the skin zone radius r_s, skin zone permeability k_s, wellbore radius r_w, and formation permeability k (Figure 2.12):

$$s = \left[\left(\frac{k}{k_s}\right) - 1\right] \ln\left(\frac{r_s}{r_w}\right). \qquad (2.24)$$

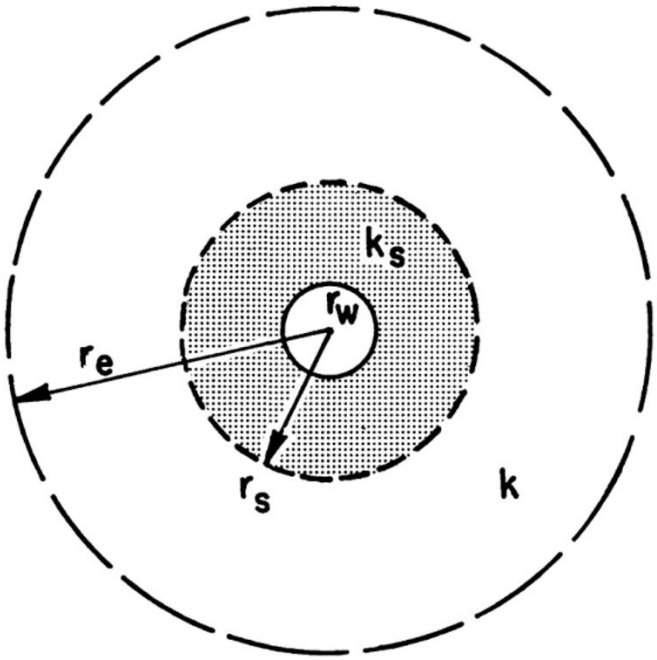

Figure 2.12: A schematic of well with a damaged zone (skin damage) (Joshi, 1991).

2.5.3 Skin Damage for Horizontal Wells

Often skin factors are estimated using drill stem testing or pressure build-up tests (Joshi, 1991). Once skin factors are known, pressure drops across the damaged zone can be estimated from reformulating Equation 2.23. The vertical well pressure drops in the skin region can then be expressed as

$$(\Delta p)_{skin} = s(\frac{141.2\mu_o B_o}{k})(\frac{q}{h}). \qquad (2.25)$$

As can be seen from Equation 2.25, $(\Delta p)_{skin}$ depends on q/h, the rate of fluid entry per unit length of the wellbore. Similarly, for horizontal wells, skin pressure drops can be approximated as

$$(\Delta p)_{skin} = s(\frac{141.2\mu_o B_o}{k})(\frac{q}{L}). \qquad (2.26)$$

Since the rate of fluid entry into wellbore per unit length of a horizontal well is much smaller than that of a vertical well, the pressure loss in the skin region in a horizontal well is also smaller than that in a vertical well, for a given positive skin factor s. Correspondingly, for a given skin damage, the stimulation treatment to remove near-wellbore damage would have less effect on the productivity of a horizontal well than on a vertical well (Joshi, 1991). However, because of the additional drilling time associated with horizontal wells, they may show much more near-wellbore damage than vertical wells, especially when drilling in low-permeability reservoirs (Joshi, 1991). Therefore, proper procedures must be adopted to cleanup and/or minimize the damage.

2.5.4 Effect of Anisotropy

The discussion in previous sections is restricted to reservoirs with homogeneous and isotropic permeabilities where $k_x = k_y$. However, in reality, such reservoirs may never exist. Therefore, it is important to consider the effects of anisotropy. For instance, as shown in Figure 2.13, in a naturally fractured reservoir, the permeability along fractures is larger than the permeability perpendicular to fractures. In this case, a vertical well would drain more length along the direction of the fractures (Joshi, 1991). More specifically, Joshi (1991) pointed out that an areally anisotropic reservoir would be the equivalent of a reservoir with an effective horizontal permeability of $\sqrt{k_x k_y}$, and the length along the high-permeability side is $\sqrt{k_x/k_y}$ times the length along a low-permeability side.

However, in such anisotropic reservoirs, it is difficult to drain larger reservoir length in the low permeability direction using vertical wells (Joshi, 1991). A horizontal well drilled along the low permeability direction, on the other hand, is capable of draining a significantly larger area than a vertical well, as shown in Figure 2.14. As a result, horizontal wells can be beneficial when drilling in anisotropic and/or naturally fractured

reservoirs. Similar to a vertical well, in a fractured reservoir where permeability in one direction is higher than the other, the horizontal well would accordingly drain a larger length in the high-permeability direction by a factor of $\sqrt{k_x/k_y}$, where k_y represents the higher permeability in the vertical plane, and k_x represents lower permeability in the horizontal plane (Joshi, 1991).

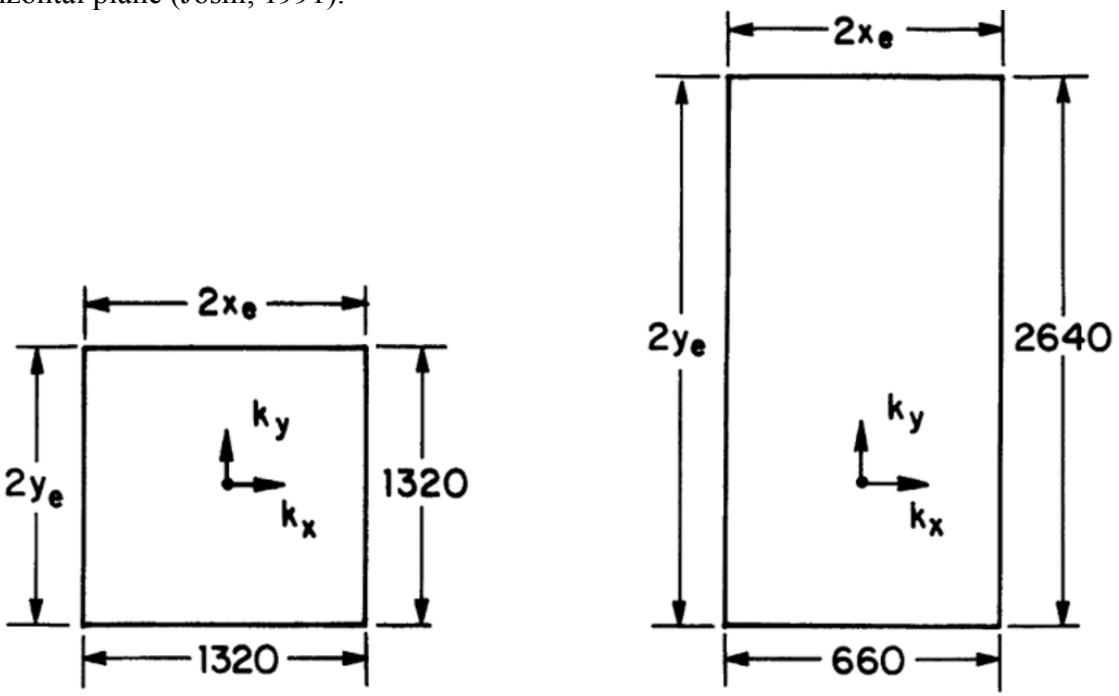

Figure 2.13: An example of drainage areas of a vertical well in isotropic and anisotropic reservoirs. (Joshi, 199)

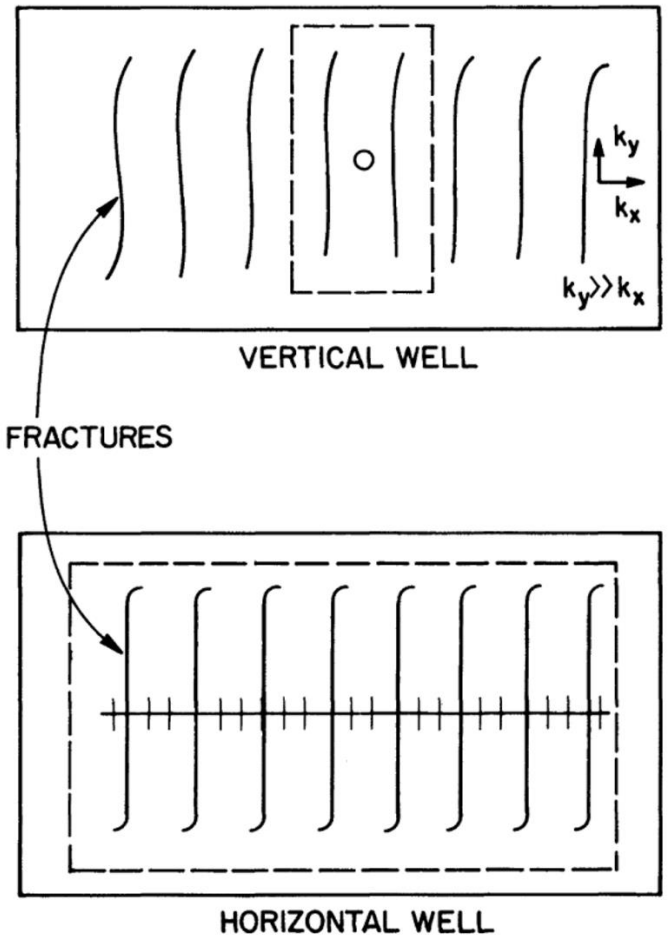

Figure 2.14: Drainage areas of horizontal and vertical wells in a fractured reservoir. (Joshi, 1991)

2.5.5 Steady-State Analytical Solutions of Horizontal Wells

Since the Hall's method is a steady-state monitoring technique, steady-state solutions of horizontal wells are reviewed in this section. As Joshi (1991) pointed out, as the simplest form of horizontal well solutions, the steady-state solutions are widely used in the industry because (1) they are easy to derive analytically; (2) it is easy to convert steady-state results to pseudo-steady state or transient results; and (3) steady-state mathematical results can be verified experimentally. In the literature, several equations are available and can be used to solve for the steady-state flow rate in a horizontal well. These solutions are summarized below.

Borisov:

$$q_h = \frac{2\pi k_h h \Delta p/(\mu_0 B_0)}{ln[(4r_{eh}/L)]+\left(\frac{h}{L}\right)\ln[\frac{h}{2\pi r_w}]}. \qquad (2.27)$$

Giger:

$$q_h = \frac{2\pi k_h L \Delta p/(\mu_0 B_0)}{(\frac{L}{h})ln\left(\frac{1+\sqrt{1-[L/(2r_{eh})]^2}}{L/(2r_{eh}}\right)+\ln[\frac{h}{2\pi r_w}]}. \qquad (2.28)$$

Renard and Dupuy:

$$q_h = \frac{2\pi k_h h \Delta p/(\mu_0 B_0)}{cosh^{-1}(X)+(\frac{h}{L})\ln[\frac{h}{2\pi r_w}]}, \qquad (2.29)$$

where X = 2a/L for ellipsoidal drainage area, a = half the major axis of drainage ellipse.

Joshi:

$$q_h = \frac{2\pi k_h h \Delta p/(\mu_0 B_0)}{ln\left[\frac{a+\sqrt{a^2-(\frac{L}{2})^2}}{L/2}\right]+\left(\frac{h}{L}\right)\ln[\frac{h}{2\pi r_w}]}, \qquad (2.30)$$

$$a = \left({}^{L}/_{2}\right)\left[0.5+\sqrt{0.25+\left(\frac{2r_{eh}}{L}\right)^4}\right]^{0.5}. \qquad (2.31)$$

From equation 2.27 to 2.31, L represents horizontal well length, h represents reservoir height, r_w represents wellbore radius, r_{eh} represents drainage radius of horizontal wells, μ_o is oil viscosity, B_o is oil formation volume factor, Δp is pressure drop from the drainage boundary to the wellbore, and q_h is flow rate of a horizontal well. All the above solutions are for isotropic reservoirs where $k_h = k_v$. Converting equation 2.30 to U.S oil field units, equation 2.30 becomes

$$q_h = \frac{0.007078 k_h h \Delta p/(\mu_0 B_0)}{ln\left[\frac{a+\sqrt{a^2-(\frac{L}{2})^2}}{L/2}\right]+\left(\frac{h}{L}\right)\ln[\frac{h}{2\pi r_w}]}, \qquad (2.32)$$

where q_h is oil flow rate in STB/day, k_h is horizontal permeability in mD, h is reservoir thickness in ft, Δp is pressure drop from the drainage radius to the wellbore in psi, μ_0 is oil viscosity in cp, B_o is formation volume factor in RB/STB, L is horizontal well length in ft, and r_w is wellbore radius in ft.

For anisotropic reservoirs where $k_h \neq k_v$, Joshi (1991) modified the steady-state equation to include the effect of reservoir anisotropy. Such a modification is shown in Equation 2.33:

$$q_h = \frac{0.007078 k_h h \Delta p/(\mu_0 B_0)}{ln\left[\frac{a+\sqrt{a^2-(\frac{L}{2})^2}}{L/2}\right]+\left(\frac{\beta h}{L}\right)\ln[\frac{\beta h}{2r_w}]}, \qquad (2.33)$$

where $\beta = \sqrt{k_h/k_v}$.

Chapter 3: Hall Plot Method for Horizontal Wells

3.1 Derivation Of Hall Plot Method For Horizontal Wells

To apply Hall's method for horizontal wells, we start with Joshi's (1991) equation for fluid flow into horizontal wells:

$$q_h = \frac{k_{rw} k h \Delta P}{141.2 \mu_w B_w \left[\ln\left(\frac{a + \sqrt{a^2 - \left(\frac{L}{2}\right)^2}}{L/2} \right) + \left(h/L\right) \ln\left(h/2r_w\right) + S \right]}, \qquad (3.1)$$

where $a = \left(L/2\right)\left[0.5 + \sqrt{0.25 + \left(\frac{2r_{eh}}{L}\right)^4}\right]^{0.5}$, and r_{eh} represents drainage radius of a horizontal well. To obtain a similar form as the original Hall's method, we integrate both sides with respect to time and get

$$W_{i-horizontal} = \frac{k_{rw} k h \int (P_{wf} - P_e) dt}{141.2\, B_w \mu_w \left[\ln\left(\frac{a + \sqrt{a^2 - \left(\frac{L}{2}\right)^2}}{L/2} \right) + \left(h/L\right) \ln\left(h/2r_w\right) + S \right]}. \qquad (3.2)$$

Rearranging and substituting Equation into 3.2, we arrive at an equation for building a Hall plot for a horizontal well:

$$\int P_{tf} dt = \frac{141.2 B_w \mu_w \left[\ln\left(\frac{a + \sqrt{a^2 - \left(\frac{L}{2}\right)^2}}{L/2} \right) + \left(h/L\right) \ln\left(h/2r_w\right) + S \right]}{k_{rw} k h} W_{i-horizontal}$$

$$+ \int (P_e - \Delta P_f + \rho g D) dt. \qquad (3.3)$$

The slope of the Hall plot for horizontal well is then

$$m_{H-horizontal} = \frac{141.2 B_w \mu_w \left[\ln\left(\frac{a+\sqrt{a^2-\left(\frac{L}{2}\right)^2}}{L/2}\right)+\left(h/L\right)\ln\left(h/2r_w\right)+S\right]}{k_{rw} kh}. \quad (3.4)$$

3.2 Simulation Model Description

During water injection, injected water may contain particles that plug the pore throats and subsequently reduce the permeability in the near-wellbore region. This reduction in permeability leads to a positive skin factor. If all the other factors remain constant, this change in skin factor, from 0 to a positive number, will increase the slope of a Hall plot. To verify Hall method's applicability on horizontal wells, reservoir simulation models are built and run using CMG. A base case with no formation damage is first constructed as a reference. Scenarios in which the presence of single skin zone and multiple skin zones in both horizontal and vertical wells are then built for comparison. The details of the simulation model are described in this section.

3.2.1 Base Case – Horizontal Well with No Formation Damage

For the base case, the reservoir is assumed to be rectangular, with a dimension of 4000 ft in the i-direction, 2400 ft in the j-direction, and 400 ft in the k-direction. The reservoir is gridded using Cartesian system, with 50 grid blocks in the i-direction, 30 grid blocks in the j-direction, and 5 grid blocks in the k-direction. The top of the reservoir is at 5000 ft below the surface. A 3D view of the reservoir is shown in Figure 3.1. Table 3.1 summarizes reservoir properties used in the base case. The reservoir rock is assumed to be water-wet and initially saturated with gas. The relative permeability correlation parameters used is shown in Table 3.2. The relative permeability curves are generated using the correlation

$$k_{rw} = k_{rwiro} \times \left[\frac{S_w - S_{wcrit}}{1 - S_{wcrit} - S_{oirw}}\right]^{N_w}$$

$$k_{rg} = k_{rgcl} \times \left[\frac{S_g - S_{gcrit}}{1 - S_{gcrit} - S_{wcon}}\right]^{N_g}$$

The relative permeability curves for water and gas are shown in Figure 3.2. The effects of capillary pressure are included. The capillary pressure curve, shown in Figure 3.3, is generated from Leverett-J function.

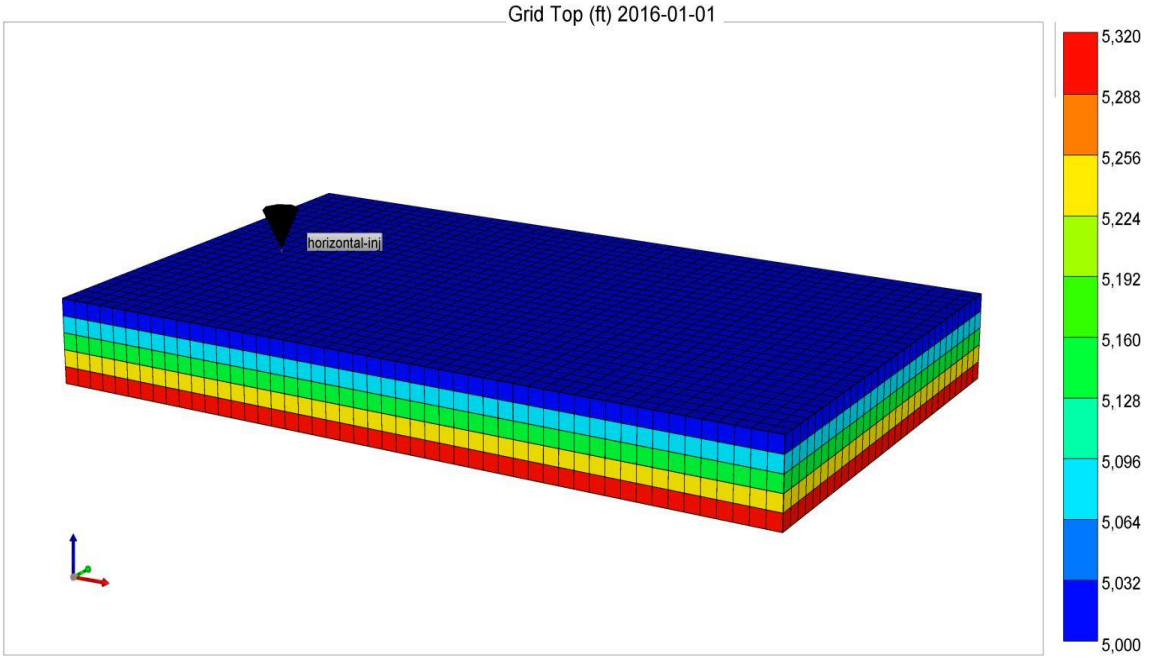

Figure 3.1: 3D view of reservoir.

Parameter	Value
Porosity	0.1
Permeability I (md)	10
Permeability J (md)	10
Permeability K (md)	10
Initial Reservoir Pressure (psi)	4000
Initial Water Saturation	0.25
Rock Compressibility (psi^{-1})	1e-6

Table 3.1: Reservoir properties for base case.

Parameter	Value
S_{wcon} – Endpoint Saturation: Connate Water	0.25
S_{wcrit} – Endpoint Saturation: Critical Water	0.25
S_{gcon} – Endpoint Saturation: Connate Gas	0.2
S_{gcrit} – Endpoint Saturation: Critical Gas	0.2
k_{rwiro} – k_{rw} at 100% water	0.8
k_{rgcl} – k_{rg} at Connate Liquid	0.8
Exponent for calculating k_{rw} from k_{rwiro}	2
Exponent for calculating k_{rg} from k_{rgcl}	2

Table 3.2: Relative permeability correlations.

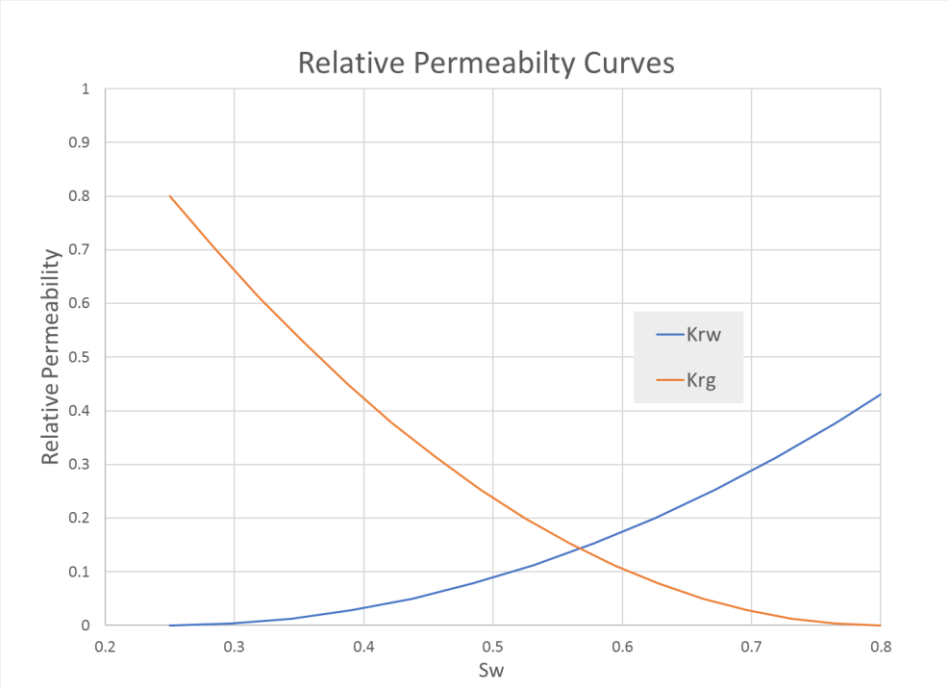

Figure 3.2: Relative permeability curves.

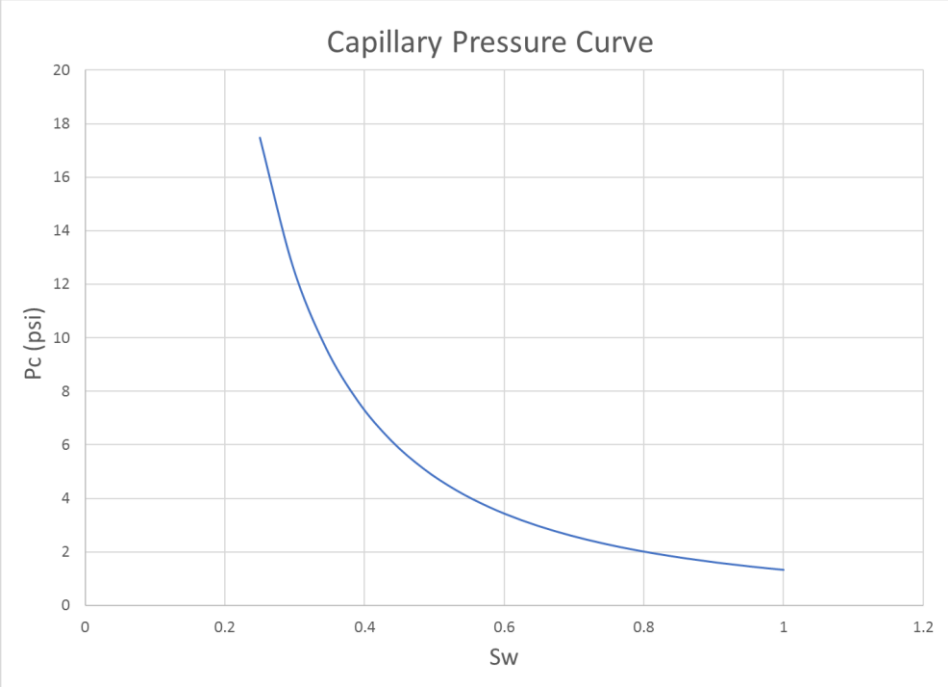

Figure 3.3: Capillary Pressure Curve.

For the base case, a horizontal injection well is built in the model. The horizontal section of the well is oriented in I direction, with a well radius of 0.25 ft. The depth of the horizontal section is located at 5,200 ft, which is in the middle of the reservoir. The well is 2,000 ft long, with a perforation spacing of 160 ft and a total of 13 perforations. The injected fluid is assumed to be water. The well is assumed to be operated with a constant surface water injection rate of 6,000 bbl/day. A 3D view of the horizontal well is shown in Figure 3.4.

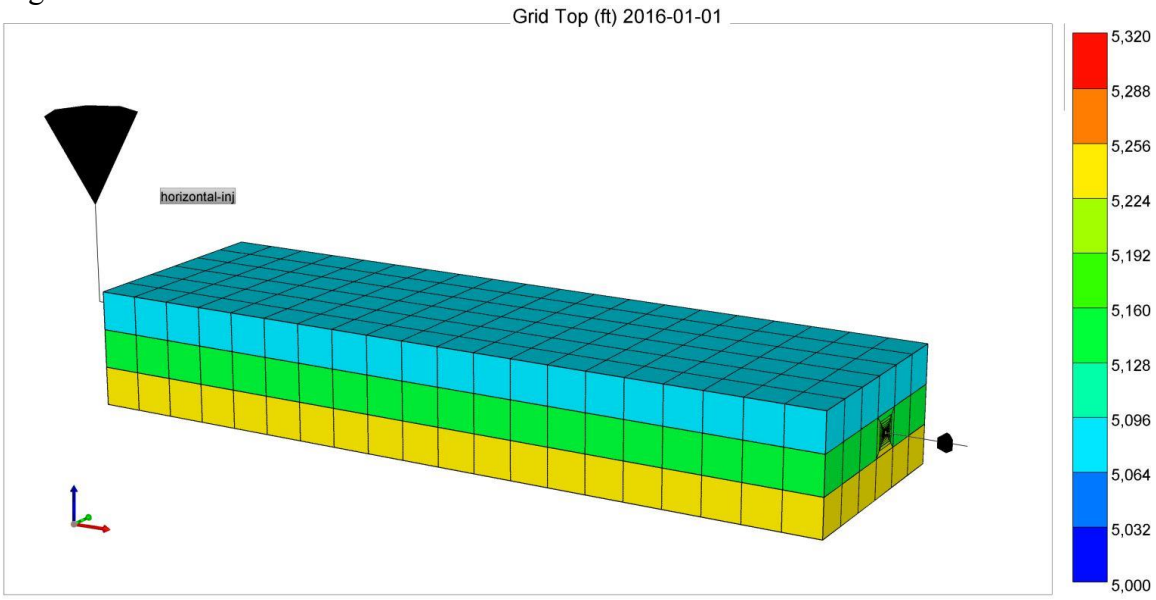

Figure 3.4: 3D view of horizontal injection well.

For the base case, it is assumed that no formation damage or stimulation is induced in the near-wellbore region. Water is injected for a total period of 10 days. Through simulation, bottom hole pressure and injected fluid volume data are generated. The data is then further analyzed using Hall's method and will be discussed in Chapter 4.

3.2.2 Damaged Case – Horizontal Well with 1 Damaged Skin Zone

As particles in the injected fluid gradually plug the pore throats, the formation is damaged, and this is reflected in a decrease in permeability in the near-wellbore region. To illustrate this reduction in permeability, a damaged case with a single damaged skin zone is constructed. The grid blocks are locally refined in the near-wellbore region, which is shown in Figure 3.5. At day 5 during water injection, a near-wellbore skin zone of reduced permeability is added. The reduced permeability zone is assumed to have a radius of 80 ft, extending from the wellbore into the formation in I, J, and K directions. Three scenarios with different extents of formation damage (25%, 50% and 75% of permeability reduction in the skin zone) are built. As stated in the base case, the undamaged permeability in the formation is 10md. The damaged permeability for the three scenarios are then 7.5md, 5md, and 2.5md, respectively. Figure 3.6 shows a 3D view of the horizontal well with a single damaged zone in the near-wellbore region. The blue region indicates the damaged skin zone.

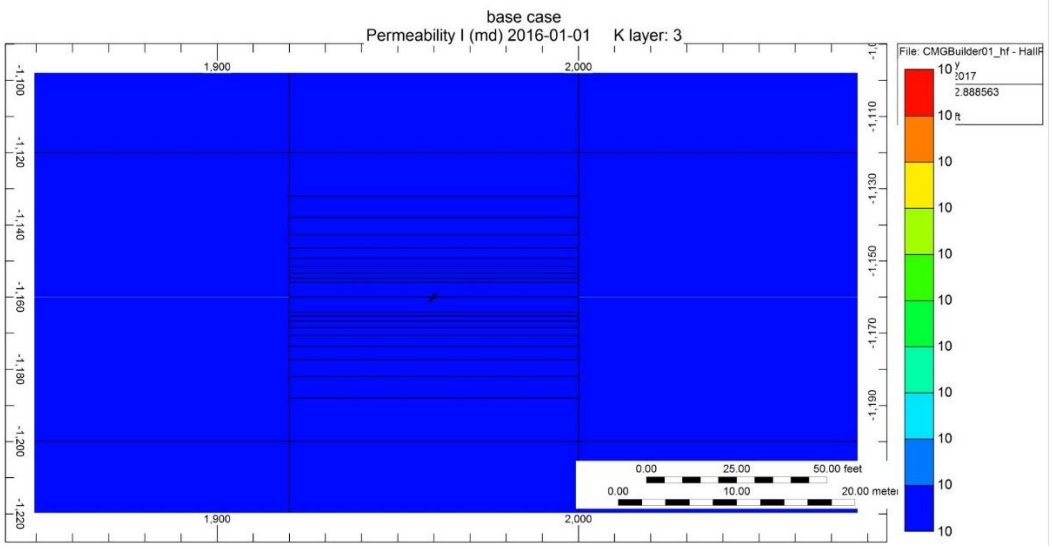

Figure 3.5: Locally refined grid in the near-wellbore region.

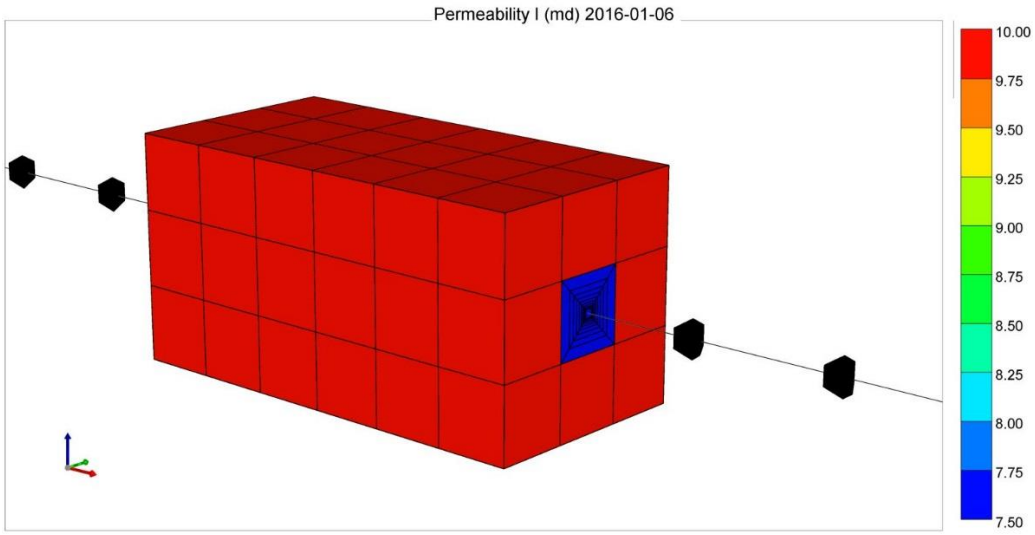

Figure 3.6: 3D view of horizontal well with 1 damaged zone.

3.2.3 Damaged Case – Horizontal Well with 2 Damaged Skin Zones

This study further investigates Hall's method's applicability on a more complicated case – damaged case with 2 skin zones. In this case, during the injection period, it is assumed that no damage occurs from day 0 to day 3; a single skin zone with permeability of 7.5 md is generated from day 3 to day 5; the permeability of this single skin zone is decreased to 5 md starting from day 5; and a second skin zone with permeability of 7.5 md is added adjacent to the original skin zone. Figure 3.7 shows a 3D view of the horizontal well with 2 damaged zones in the near-wellbore region. The red color represents the undamaged reservoir; the blue color represents the skin zone where permeability is reduced to 5 md; the green color represents the skin zone where permeability is reduced to 7.5 md. Similar to the 1 damaged zone case, the simulation is run to test Hall method's applicability on water injection with 2 damaged zones present.

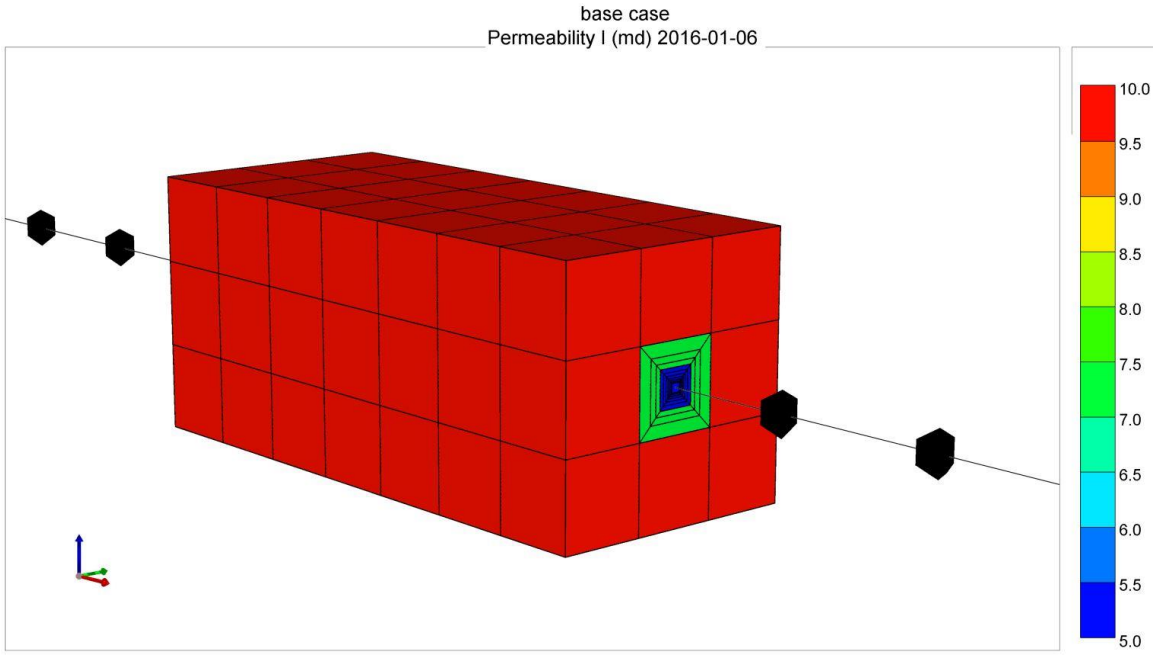

Figure 3.7: 3D view of horizontal well with 2 damaged zones.

3.2.4 Vertical Well with No Formation Damage

As stated, one of the objectives of this research is to compare the effects of skin damage between horizontal and vertical wells drilled in a similar environment by using the Hall plot method. To do so, a vertical well model is built, using the same parameters as used in the horizontal well model. A 3D view of the vertical well is shown in Figure 3.8. The well is assumed to be drilled right in the middle of reservoir. The reservoir properties remain unchanged as compared to the horizontal well cases. The depth of the vertical well is 5,400 ft. The well is producing from 5,000 ft to 5,400 ft.

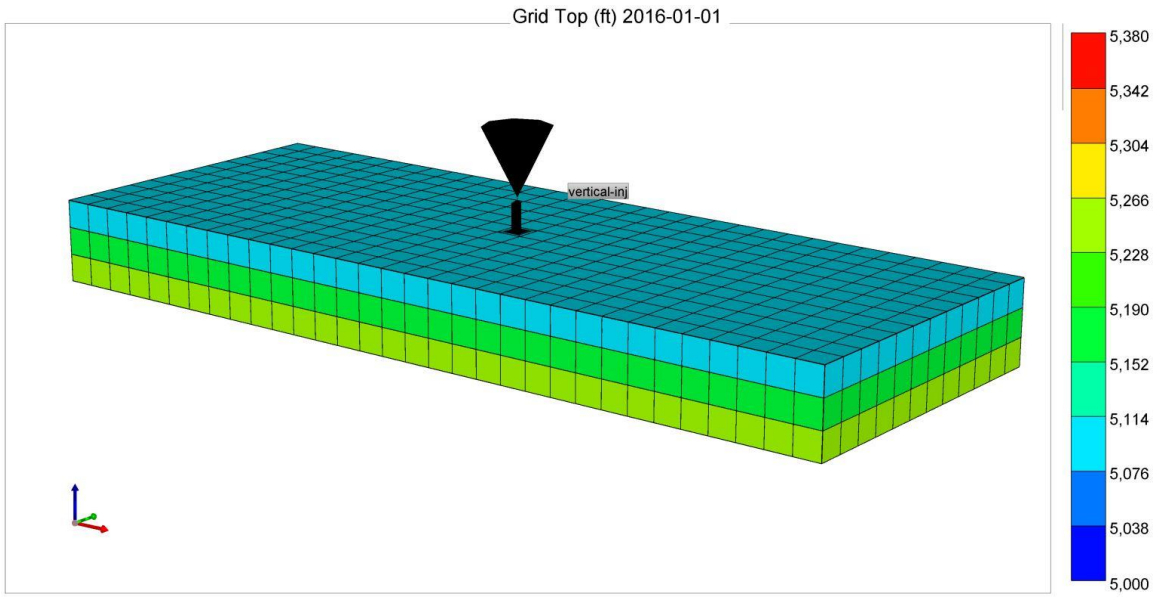

Figure 3.8: 3D view of vertical injection well.

It is assumed that no formation damage or stimulation is induced in the near-wellbore region of the vertical well. Water is injected for a total period of 10 days. Simulation results are compared with those of the horizontal well case and will be discussed in the Chapter 4.

3.2.5 Vertical Well with 1 Damaged Skin Zone

Using similar setup to that used in the damaged-horizontal well cases, a model of a vertical well with one damaged skin zone is built to investigate and compare the extent of formation damage between horizontal and vertical wells. In the same way as in the damaged-horizontal well case, at day 5 during water injection, a near-wellbore skin zone of reduced permeability is added. The reduced permeability zone is assumed to have a radius of 80 ft, extending from the wellbore into the formation in I, J, and K directions. Three scenarios with different extents of formation damage (25%, 50% and 75% of permeability reduction in the skin zone) are built. As stated in the base case, the undamaged

permeability in the formation is 10 mD. The damaged permeability for the three scenarios are then 7.5 mD, 5 mD, and 2.5 mD, respectively. Figure 3.9 shows a cross-sectional view of the vertical well with one damaged zone in the near-wellbore region. The blue region indicates the damaged skin zone.

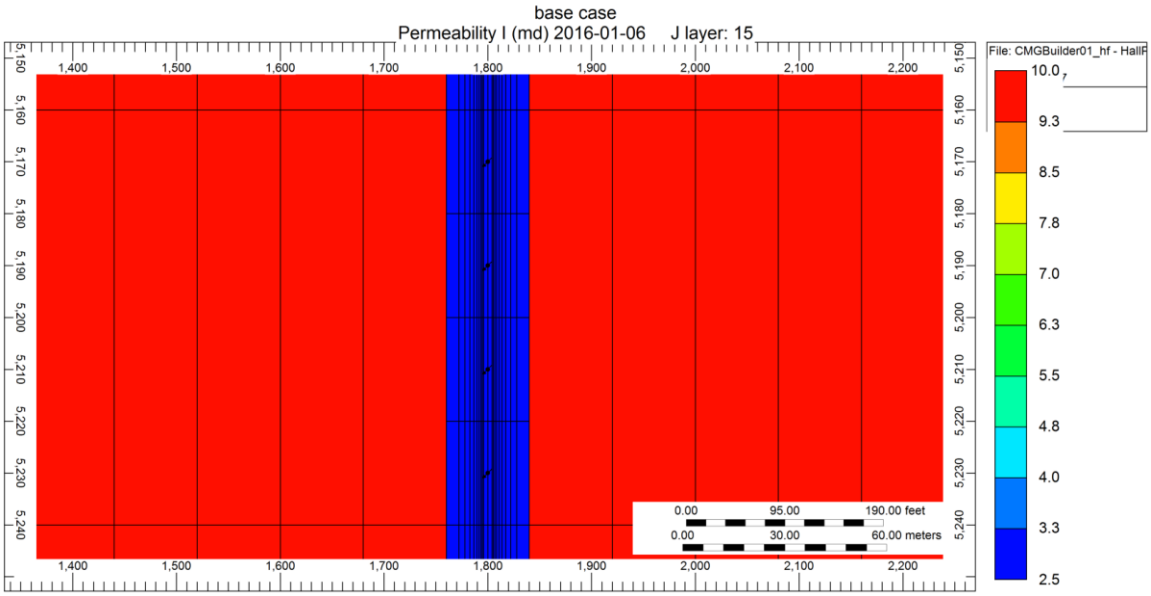

Figure 3.9: Cross-sectional view of the vertical well with 1 damaged zone.

3.2.6 Vertical Well with 2 Damaged Skin Zones

Following the case of damaged-horizontal well with two skin zones, a vertical well model with the same formation damage scenarios is built. Similarly, in this case, during the injection period, it is assumed that no damage occurs from day 0 to day 3; a single skin zone with permeability of 7.5 mD is generated from day 3 to day 5; the permeability of this single skin zone is decreased to 5 mD starting from day 5; and a second skin zone with permeability of 7.5 mD is added adjacent to the original skin zone. Figure 3.10 shows a cross-sectional view of the vertical well with 2 damaged zones in the near-wellbore region. The red color represents the undamaged reservoir; the blue color represents the skin zone

where permeability is reduced to 5 mD; the green color represents the skin zone where permeability is reduced to 7.5 mD.

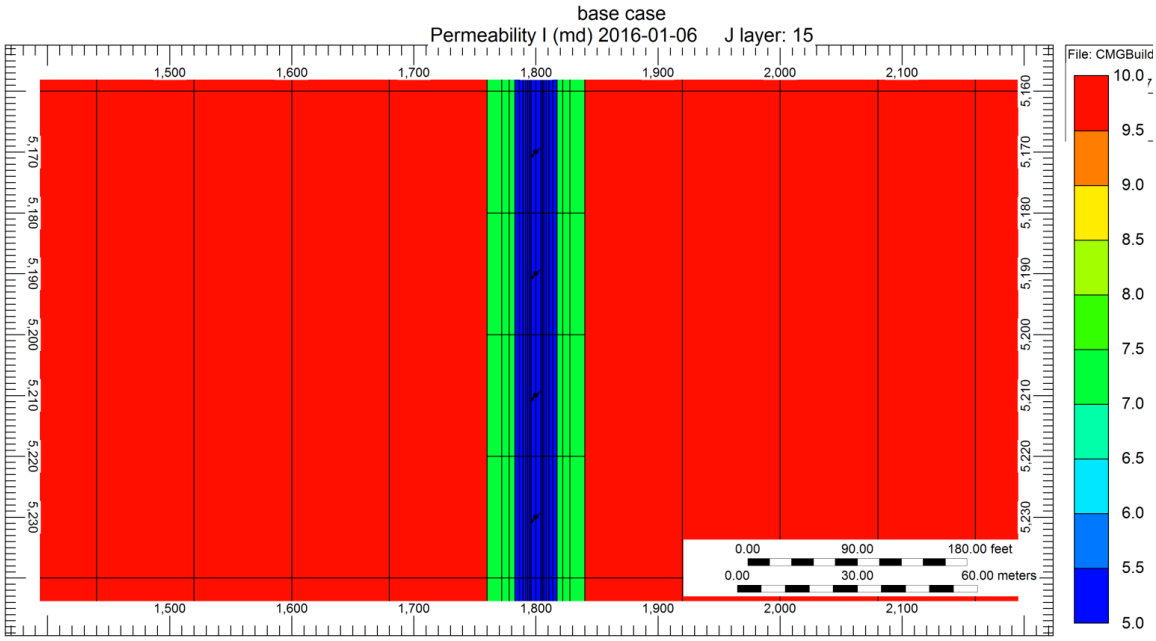

Figure 3.10: Cross-sectional view of the vertical well with 2 damaged skin zones.

Chapter 4: Results and Discussion

4.1 Analyzing Horizontal Well Injectivity Using Hall Plot

4.1.1 Base Case – Horizontal Well with No Formation Damage

As stated in Chapter 3, a base case of a horizontal well with no formation damage was built and run to generate pressure and water injection data. The simulation was run assuming a water injection period of 10 days with a rate of 6,000 bbl/day. To produce a Hall plot for the base case, the pressure integral with respect to time was calculated and plotted against the cumulative water injection volume, as shown in Figure 4.1. A linear relationship was used to fit the data points. After fitting the data, the Hall plot slope was calculated to be 0.74 for the base case. The straight line, or constant slope, indicates that the horizontal well's injectivity remains unchanged, which corresponds to the undamaged scenario with a skin factor of 0.

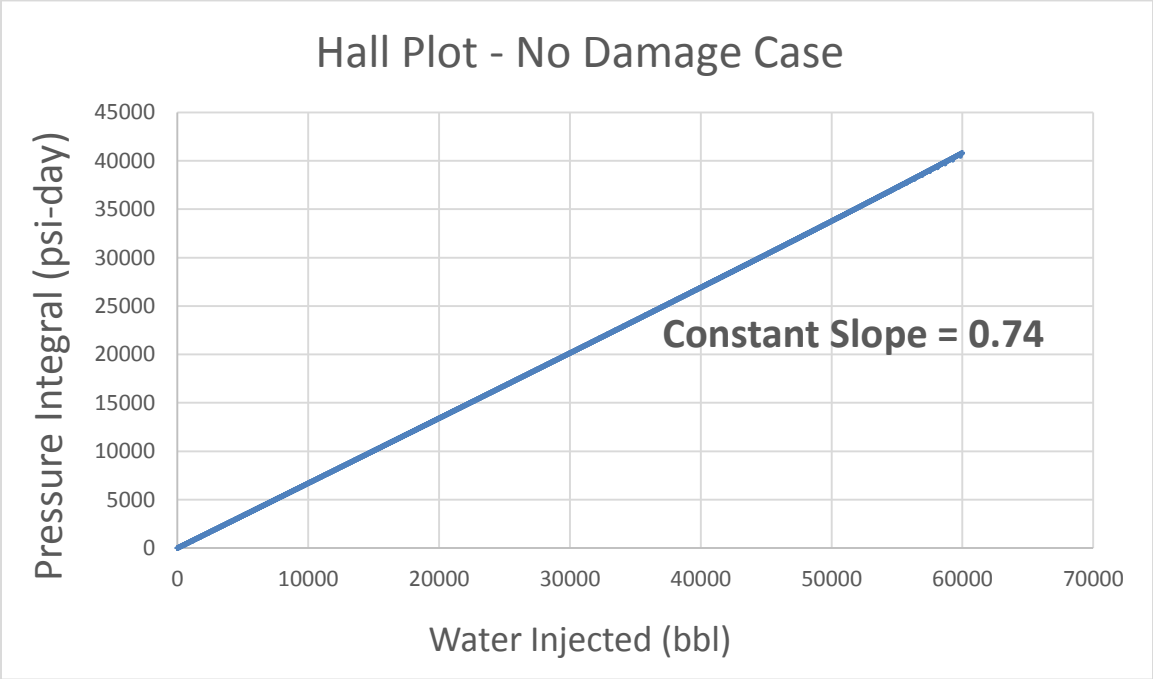

Figure 4.1: Hall plot for horizontal well without damage.

4.1.2 Damaged Case – Horizontal Well with 1 Damaged Skin Zone

For the damaged horizontal well cases, the simulation was run to generate pressure and rate data, which were plotted using the Hall plot method. For the 1 skin zone case, three scenarios – 25%, 50%, and 75% permeability reduction in the near-wellbore region – were investigated. As shown in Figure 4.2, as the horizontal well becomes damaged, an increase in the Hall slope is observed in all three scenarios. Also, as the extent of formation damage increases, the Hall slope becomes larger. Table 4.1 summarizes the calculated Hall slope values for the three scenarios as compared to the undamaged case. Since all the parameters except for the skin factor remain unchanged across the three scenarios, the change in Hall slope can be seen as a direct indication of change in skin factor, in other words, formation damage. Therefore, the results demonstrate that the Hall plot method can be used to analyze changes in the horizontal well's injectivity due to formation damage.

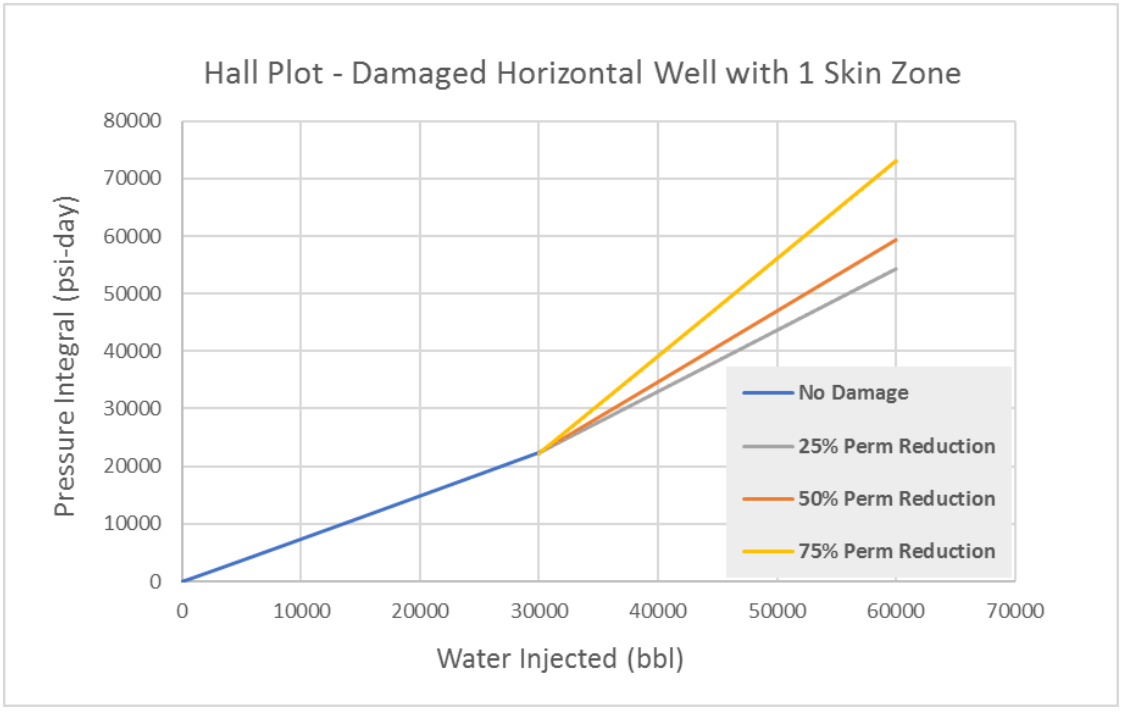

Figure 4.2: Hall plot – damaged horizontal well with 1 skin zone.

Case	Hall Slope
No damage	0.74
25% permeability reduction	1.06
50% permeability reduction	1.23
75% permeability reduction	1.69

Table 4.1: Hall slopes for horizontal well with 1 skin zone.

4.1.3 Damaged Case – Horizontal Well with 2 Damaged Skin Zones

The study further investigates the use of the Hall plot in a horizontal well with multiple damaged skin zones. As described in Section 3.2.3, a damaged case with two skin zones was built and run. The pressure integral and cumulative water injection data were plotted using the Hall plot method, as shown in Figure 4.3. Table 4.2 summarizes the calculated Hall slopes of the 2 skin zones case. An increase in Hall slope is observed when the undamaged horizontal well becomes damaged with 1 skin zone. As the damage radius increases and a second skin zone is generated, and another slight increase in the Hall slope is observed. However, in reality, where the permeability profile in the near-wellbore region is much more complex and skin zones are less distinguishable, the changes in Hall slope cannot be simply interpreted as a change in the number of skin zones. In fact, the value of the Hall slope is a combinational effect of multiple reservoir parameters as well as the skin factor. Therefore, to give more precise interpretation of the injectivity of a horizontal well, additional measures, along with the Hall plot method, need to be considered.

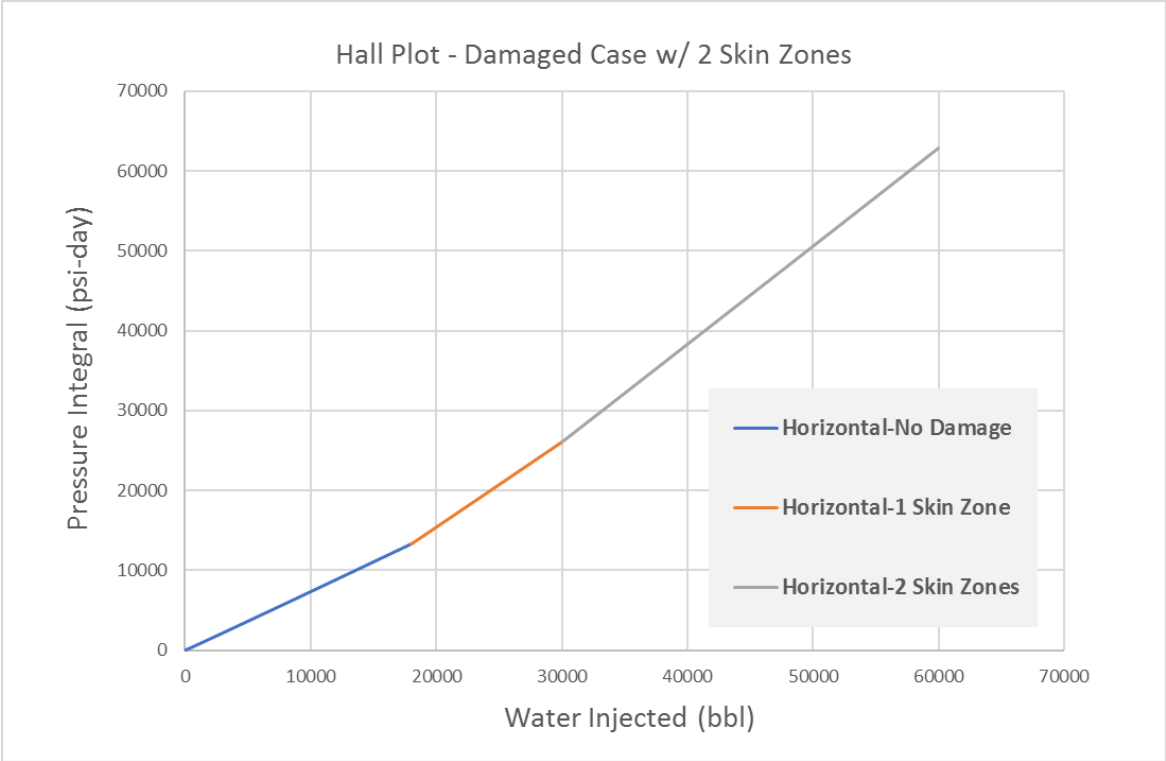

Figure 4.3: Hall plot – damaged case with 2 skin zones.

Case	Hall Slope
No damage	0.74
1 Skin Zone	1.06
2 Skin Zones	1.23

Table 4.2: Hall slopes for horizontal well with 2 skin zones.

4.2 COMPARISON OF HORIZONTAL VS. VERTICAL WELL INJECTIVITY USING HALL PLOTS

4.2.1 Hall Plots for Damaged Vertical Well

As stated in Chapter 2, since the rate of fluid entry into the wellbore per unit length of a horizontal well is much smaller than that of a vertical well, the pressure loss in the skin region in a horizontal well is also smaller than that in a vertical well, for a given positive skin factor s. Here, the study extends to a comparison of horizontal versus vertical well injectivity using the Hall plot method. As described in Section 3.2.4 – 3.2.6, simulations were run for vertical well with no formation damage, 1 skin zone, and 2 skin zone cases. The pressure integral and water injection data were plotted using Hall plot method, as shown in Figure 4.4 and 4.5. The Hall slopes are summarized in Table 4.1 and Table 4.2. Similar to the horizontal well cases, increases in Hall slopes are observed when the extent of formation damage and/or number of skin zones increases.

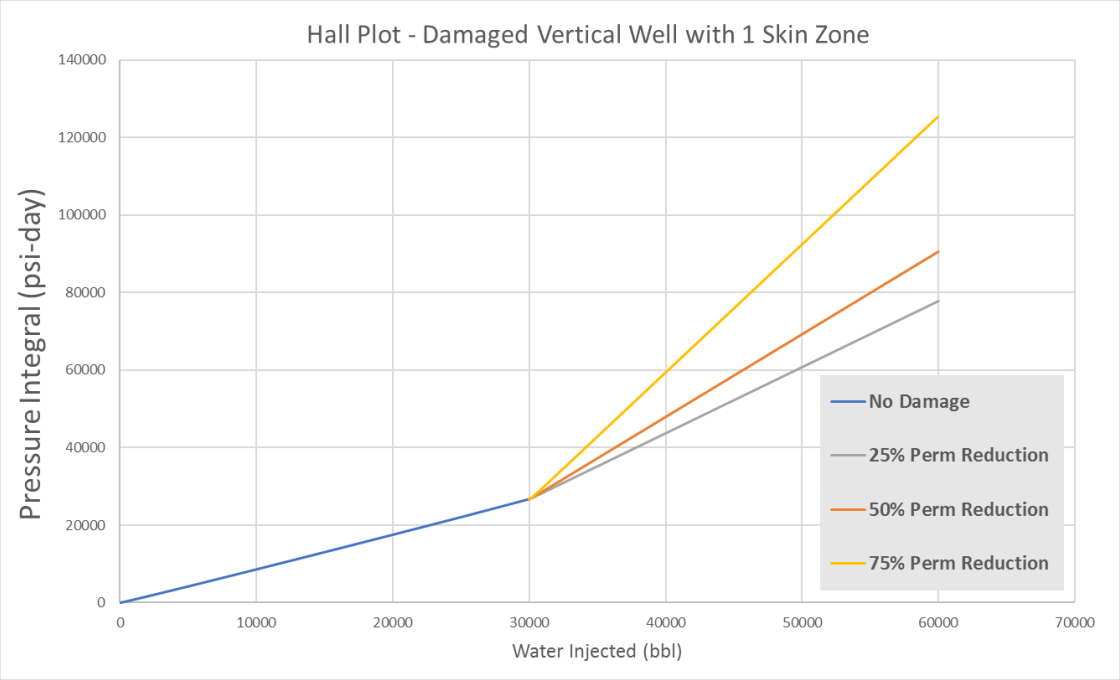

Figure 4.4: Hall plot – damaged vertical well with 1 skin zone.

Case	Hall Slope
No damage	0.89
25% permeability reduction	1.71
50% permeability reduction	2.13
75% permeability reduction	3.30

Table 4.3: Hall slopes for vertical well with 1 skin zone.

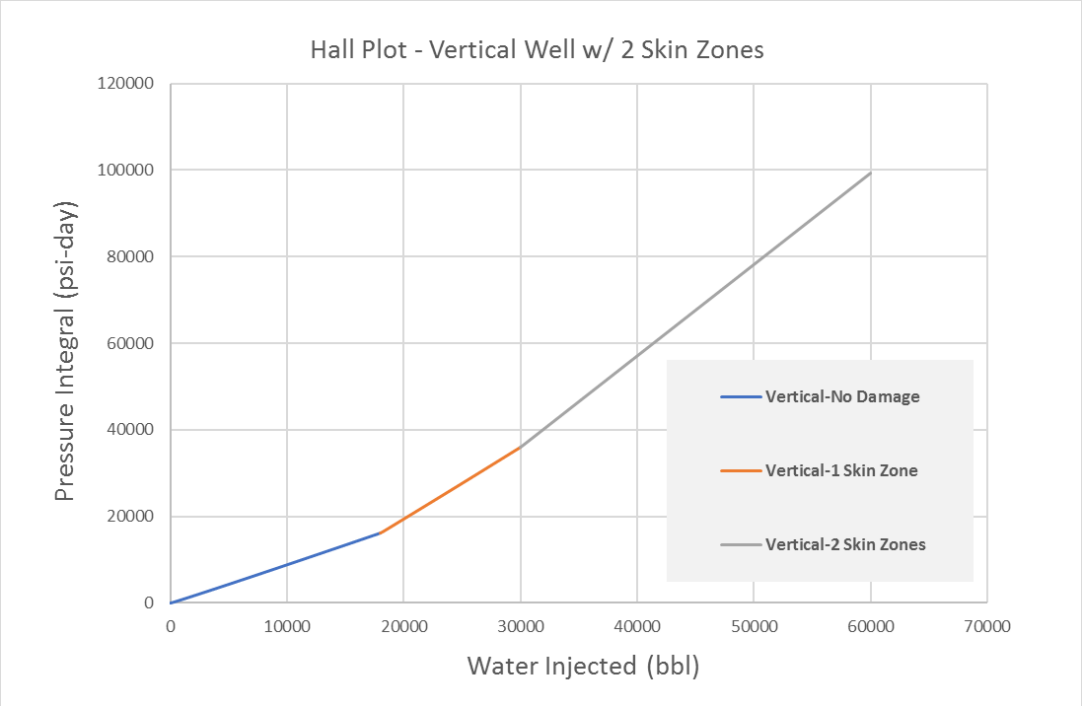

Figure 4.5: Hall plot – vertical well with 2 skin zones.

Case	Hall Slope
No Damage	0.89
1 Skin Zone	1.67
2 Skin Zones	2.11

Table 4.4: Hall slopes for vertical well with 2 skin zones.

4.2.2 Skin factors of horizontal vs. vertical wells

To compare the injectivity between horizontal well and vertical wells, pressure and water injection data were plotted on the same Hall plot for both wells and for both 1 skin zone and 2 skin zones cases, as shown in Figure 4.6 and 4.7. As shown in the two figures, vertical wells shown steeper Hall slopes than horizontal well for all cases. The percentages of increase in Hall slopes were calculated. Using the Hall slopes determined from the plot and reservoir parameters used in the simulation models, skin factors for all cases were calculated and summarized in Table 4.5 and 4.6.

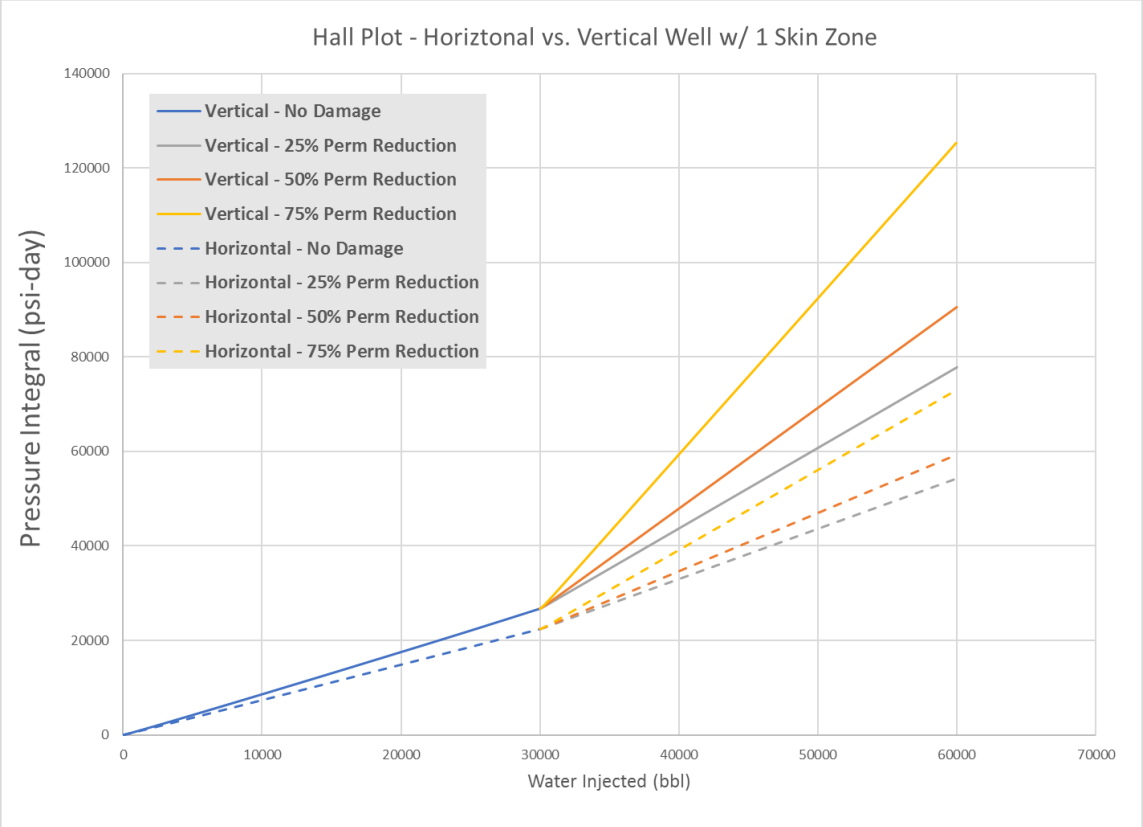

Figure 4.6: Hall plot – horizontal vs. vertical well with 1 skin zone.

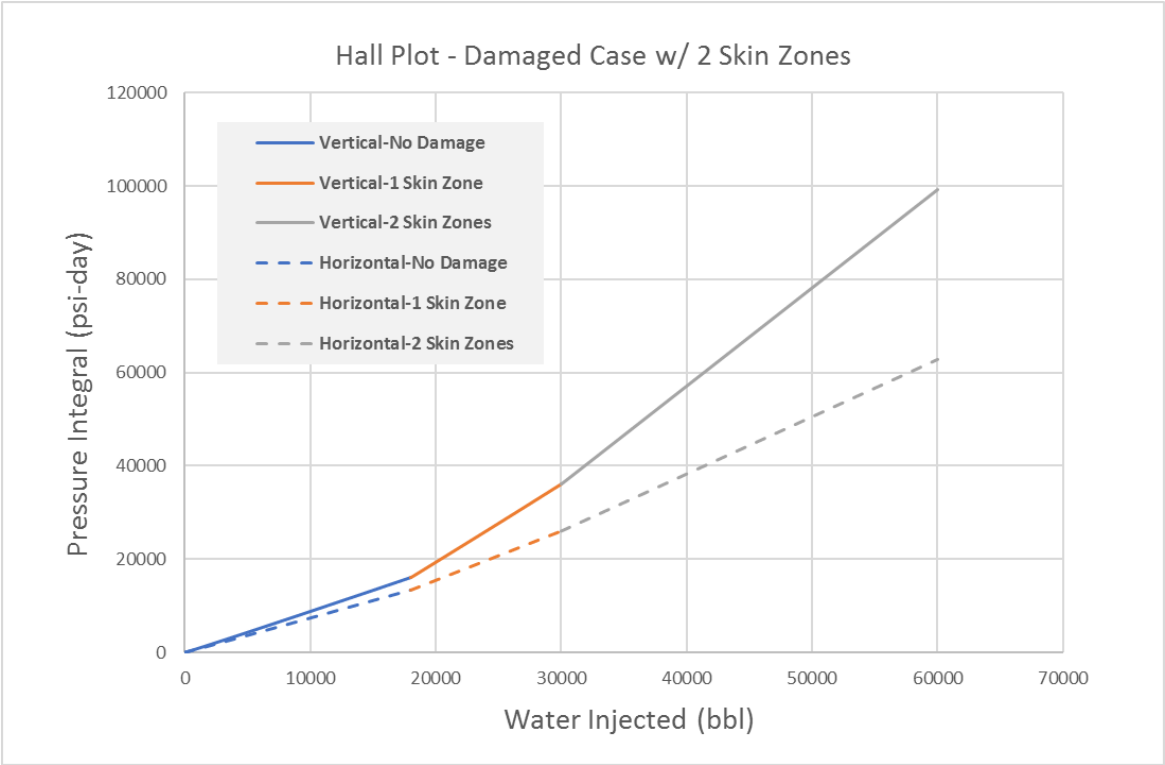

Figure 4.7: Comparison of Hall plots between horizontal and vertical wells.

Case	Vertical Well Hall Slope	% Change in Slope	Calculated Skin	Horizontal Well Hall Slope	% Change in Slope	Calculated Skin
No Damage	0.89	-	0	0.74	-	0
25% Perm Reduction	1.71	92.1%	17.4	1.06	43.2%	6.8
50% Perm Reduction	2.13	139.3%	26.3	1.23	66.2%	10.4
75% Perm Reduction	3.30	270.8%	51.2	1.69	128.4%	20.2

Table 4.5: Calculated skin for damaged vertical and horizontal wells with 1 skin zone.

Case	Vertical Well Hall Slope	% Change in Slope	Calculated Skin	Horizontal Well Hall Slope	% Change in Slope	Calculated Skin
No Damage	0.89	-	0	0.74	-	0
1 Skin Zone	1.67	67.1%	16.6	1.06	43.2%	6.8
2 Skin Zones	2.106	136.6%	25.8	1.23	66.2%	10.4

Table 4.6: Calculated skin for damaged vertical and horizontal wells with 2 skin zones.

Given the same reservoir and fluid parameters, it is observed that vertical wells tend to be more damaged than horizontal wells in terms of skin factors and Hall slopes in all cases. For the 1 skin zone cases, as a vertical well becomes damaged, the percentage increase in its Hall slope and skin factor are more than twice than those of a horizontal well. Similarly, for the 2 skin zone cases, a vertical well is also observed to be more damaged than a horizontal well. This simulation result is consistent with Joshi's statement that, for a given positive skin factor, the pressure loss in the skin region in a horizontal well is smaller than that in a vertical well (Joshi, 1991). For the same reason, in reality, the stimulation treatment that is used to remove formation damage in horizontal wells may be less effective than in a vertical well drilled in the same environment. Therefore, it is important to optimize drilling design, minimize formation damage, and carefully select stimulation treatment for a horizontal well.

4.2.3 Effect of anisotropy

As discussed in Chapter 2, anisotropy in permeability can influence a well's productivity. Here, the study takes anisotropy in horizontal and vertical wells into consideration. Simulation cases were constructed for anisotropic cases where the vertical permeability is several orders of magnitude smaller than the horizontal permeability. Similar to the isotropic cases, pressure integral and water injection data were plotted using

the Hall plot method. Figure 4.8 and 4.9 show the Hall plots for horizontal and vertical wells drilled in isotropic and anisotropic reservoirs where $k_v = 0.1k_h$ and $k_v = 0.01k_h$; k_v and k_h represent the permeability in vertical and horizontal directions, respectively. Table 4.7 and 4.8 summarizes the calculated Hall slopes and corresponding skin factors for these cases. As shown in Table 4.7, the Hall slopes only change minimally when an anisotropic reservoir becomes damaged, indicating minimal changes in water injectivity. Also, the calculated skin factors for damaged anisotropic reservoirs are also smaller than those of an isotropic reservoir. This indicates that, when drilling horizontal wells in an anisotropic reservoir where vertical permeabilities are several magnitudes smaller than horizontal permeabilities, formation damage does not significantly affect water injectivity. On the other hand, as can be seen from the increase in Hall slopes when the permeability in the vertical direction decreases from $0.1k_h$ to $0.01k_h$, water injectivity also decreases. This indicates that anisotropy does have an effect on a horizontal well's water injectivity.

For a vertical well, the Hall plots in Figure 4.9 show that there is no injectivity difference between isotropic and anisotropic cases. In fact, the Hall plots of the three cases lie right on top of each other, indicating that the reduce of permeability in the vertical direction does not directly affect the injectivity of a vertical well. However, the results shown in Figure 4.9 assume that the direction of fluid flow is normal to the wellbore. When coning in the near-wellbore region occurs, fluid will flow in both vertical and horizontal directions. In this case, anisotropy could have an impact on the injectivity of a vertical well. More specifically, vertical wells usually exhibit a high pressure drawdown in the near-wellbore region; and this pressure drawdown is one of the main reasons for water coning. Horizontal wells, on the other hand, show much less pressure drawdown and less tendencies of vertical flow in the vicinity of the wellbore than vertical wells. As a result,

horizontal wells could be more preferable than vertical wells in minimizing coning and sustaining high oil and gas production rates.

It is important to note that the anisotropic simulation models assume that vertical permeabilities are smaller than horizontal permeabilities. This could represent scenarios where a reservoir is naturally fractured, with natural fractures being in the horizontal direction. In this case, a horizontal well drilled parallel to the natural fractures would not be as effective as a vertical well that is perpendicular to the natural fractures. However, if the natural fractures are oriented in the vertical direction ($k_v > k_h$), a horizontal well could drain more areas than a vertical well. In addition, the study already shown that horizontal well water injectivity only changes minimally when an anisotropic reservoir becomes damaged. Therefore, in this case, drilling a horizontal well could be much more beneficial than a vertical well in terms of drainage area as well as water injectivity.

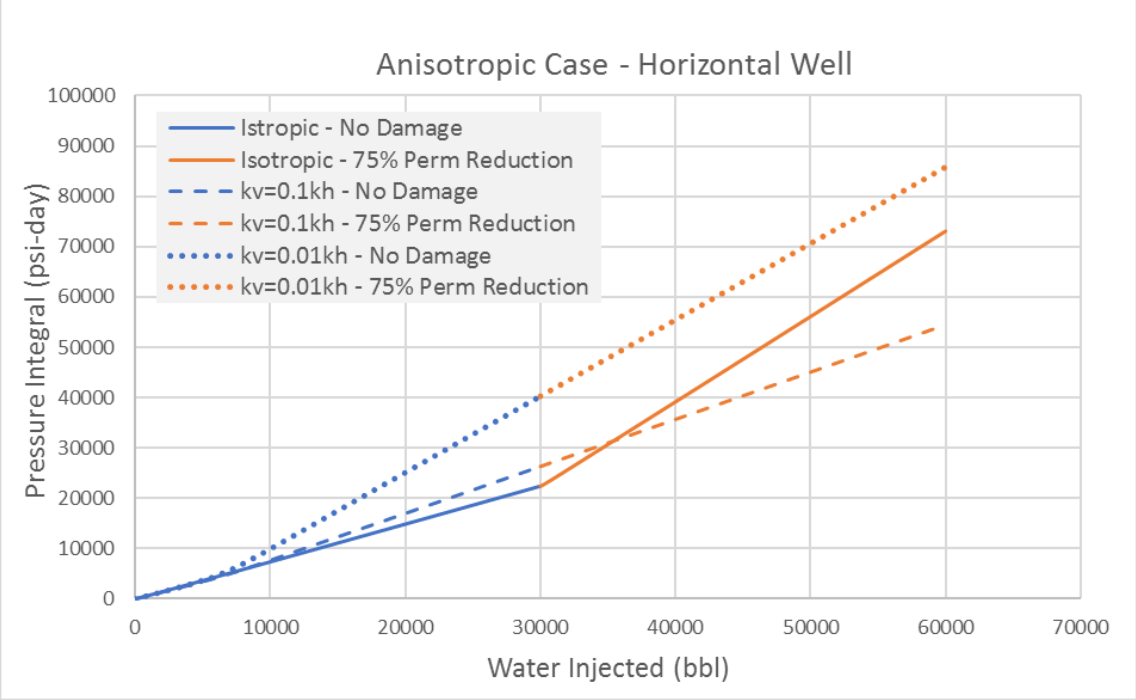

Figure 4.8: Comparison of Hall plots between isotropic and anisotropic horizontal wells.

Case	Hall Slope	Calculated Skin
Isotropic – No Damage	0.74	0
Isotropic – 75% Perm Reduction	1.69	20.2
$k_v=0.1k_h$ – No Damage	0.90	0
$k_v=0.1k_h$ – 75% Perm Reduction	0.94	0.86
$k_v=0.01k_h$ – No Damage	1.42	0
$k_v=0.01k_h$ – 75% Perm Reduction	1.52	2.12

Table 4.7: Calculated Hall slopes for isotropic and anisotropic horizontal wells.

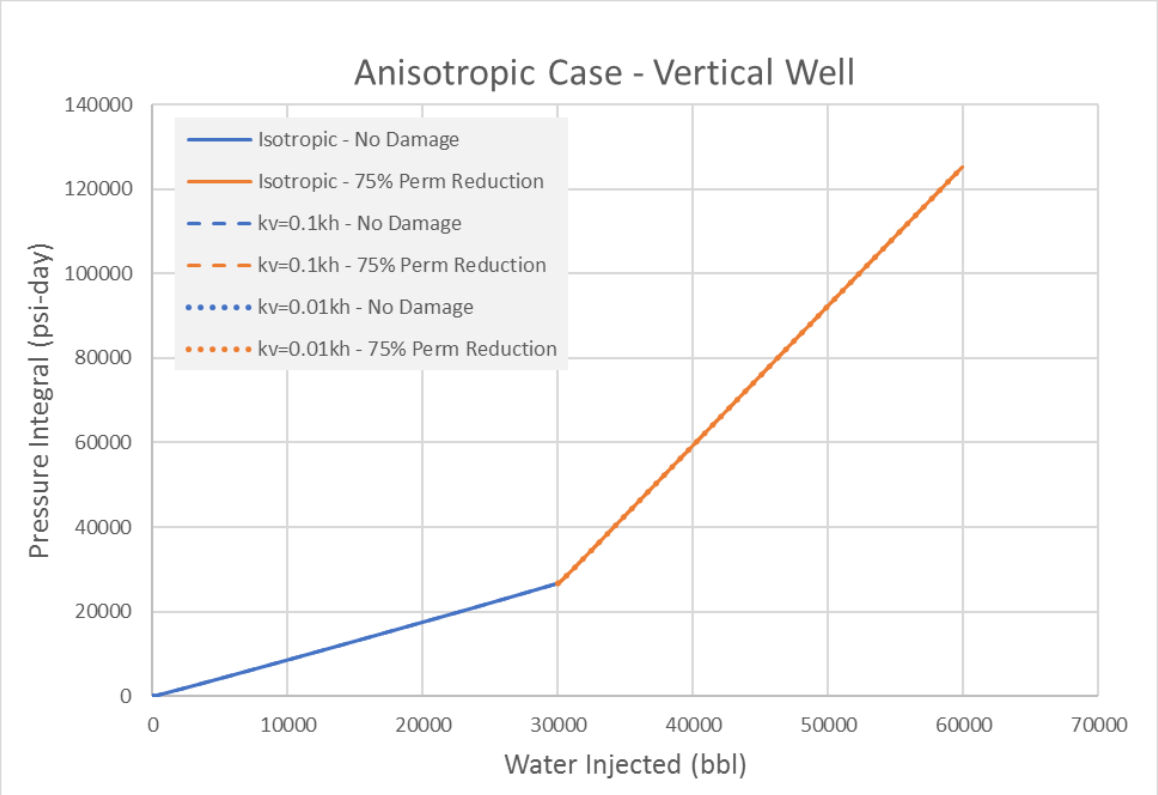

Figure 4.9: Comparison of Hall plots between isotropic and anisotropic vertical wells.

Chapter 5 Summary and Conclusions

In this research, the background, applications, and modifications of the Hall plot method were first revisited, followed by a formulation of the Hall plot method for horizontal wells. To verify the applicability of the method, numerical simulation models were built and run in CMG. The results show that –

- The Hall plot method can be used to analyze changes in horizontal well's injectivity due to formation damage.
- The number of skin zones in the near-wellbore region cannot be directly captured in the changes in Hall slopes. The value of the Hall slope is a combinational effect of multiple reservoir parameters as well as the skin factor. To give more precise interpretation of the injectivity of a horizontal well, additional measures, along with the Hall plot method, need to be considered.
- Given the same reservoir and fluid parameters, vertical wells tend to be more damaged than horizontal wells in terms of skin factors and Hall slopes. As a result, the stimulation treatment that is used to remove formation damage in horizontal wells may be less effective than in a vertical well drilled in the same environment.
- Horizontal well water injectivity only changes minimally when an anisotropic reservoir becomes damaged. When drilling in an anisotropic and/or naturally fractured reservoir where vertical permeabilities are greater than horizontal permeabilities, drilling a horizontal well could be much more beneficial than a vertical well in terms of minimizing water coning and improving injectivity.

Nomenclatures

B_w	water formation volume factor
B_o	oil formation volume factor
h	reservoir thickness
k	absolute permeability
k_s	skin zone permeability
k_x, k_h	permeability in horizontal direction
k_y, k_v	permeability in vertical direction
k_{rw}	water relative permeability
k_{rwiro}	k_{rw} at 100% water
k_{rg}	gas relative permeability
k_{rgcl}	k_{rg} at connate liquid
L	well length
N_w	exponent for calculating k_{rw}
N_g	exponent for calculating k_{rg}
P_{tf}	surface pressure
P_{wf}	wellbore pressure
P_e	reservoir pressure
q	flow rate
q_h	flow rate in a horizontal well
r_{b1}	interface between oil and water banks
r_w	wellbore radius
r_e	radius at water-oil front
r_{eh}	drainage radius of a horizontal well

r_s skin zone radius

s skin factor

S_w water saturation

S_{wcrit} endpoint saturation: critical water

S_{oirw} endpoint saturation: connate water

W_i cumulative water injected

Greek Symbols

μ fluid viscosity

ρ fluid density

ϕ matrix porosity

ΔP pressure difference

References

Alyan, M., Al Tamimi, M., Al Zinati, O., Calarasu, D., Martin, J., & Irwin, D. (2016, November 7). Mitigating Water Injectivity Decline in Tight Carbonates due to Suspended Particles. Society of Petroleum Engineers. doi:10.2118/183222-MS

Amedu, J., & Nwokolo, C. (2013, August 5). Improved Well and Reservoir Production Performance in Waterflood Reservoirs-Revolutionalizing the Hall Plot. Society of Petroleum Engineers. doi:10.2118/167602-MS

Buell, R. S., Kazemi, H., & Poettmann, F. H. (1990, February 1). Analyzing Injectivity of Polymer Solutions With the Hall Plot. Society of Petroleum Engineers. doi:10.2118/16963-PA

Hall, H. N. (1963). How to analyze waterflood injection well performance. *World Oil,* 128-130.

Hawe, D. E. (1976, January 1). Direct Approach Through Hall Plot Evaluation Improves The Accuracy Of Formation Damage Calculations And Eliminates Pressure Fall-Off Testing. Society of Petroleum Engineers.

IMEX User Guide. (2014). Computer Modeling Group.

Izgec, B., & Kabir, C. S. (2007, January 1). Real-Time Performance Analysis of Water-Injection Wells. Society of Petroleum Engineers. doi:10.2118/109876-MS

Izgec, B., & Kabir, S. (2011, February 1). Identification and Characterization of High-Conductive Layers in Waterfloods. Society of Petroleum Engineers. doi:10.2118/123930-PA

Izgec, B. (2015, September 28). Integrated Injection Modeling. Society of Petroleum Engineers. doi:10.2118/174840-MS

Jarrell, P. M., & Stein, M. H. (1991, January 1). Maximizing Injection Rates in Wells Recently Converted to Injection Using Hearn and Hall Plots. Society of Petroleum Engineers. doi:10.2118/21724-MS

Joshi, S. D. (1991). *Horizontal well technology*. Tulsa, OK: PennWell Pub.

Ojukwu, K. I., & van den Hoek, P. J. (2004, January 1). A New Way to Diagnose Injectivity Decline During Fractured Water Injection By Modifying Conventional Hall Analysis. Society of Petroleum Engineers. doi:10.2118/89376-MS

Silin, D. B., Holtzman, R., & Patzek, T. W. (2005, January 1). Monitoring Waterflood Operations: Hall Method Revisited. Society of Petroleum Engineers. doi:10.2118/93879-MS

Talabi, O. A. (2016, March 22). Modifying the Hall Plot for Analysis of Immiscible Gas Injection Wells. Offshore Technology Conference. doi:10.4043/26649-MS

Van Everdingen, A. F., & Hurst, W. (1949, December 1). The Application of the Laplace Transformation to Flow Problems in Reservoirs. Society of Petroleum Engineers. doi:10.2118/949305-G